

# Supplementary Material

Formation and transformation of Fe(III)- and Ca-precipitates in aqueous solutions and effects on phosphate retention over time

*Ville V. Nenonen<sup>1,2</sup>, Ralf Kaegi<sup>1</sup>, Stephan J. Hug<sup>1</sup>, Jörg Göttlicher<sup>3</sup>,  
Stefan Mangold<sup>3</sup>, Lenny H.E. Winkel<sup>1,2</sup>, Andreas Voegelin<sup>1,\*</sup>*

<sup>1</sup> Eawag, Swiss Federal Institute of Aquatic Science and Technology,  
Überlandstrasse 133, CH-8600 Dübendorf, Switzerland.

<sup>2</sup> ETH Zurich, Institute of Biogeochemistry and Pollutant Dynamics, Universitätstrasse  
16, CH-8092 Zürich, Switzerland.

<sup>3</sup> Karlsruhe Institute of Technology, Institute for Photon Science and Synchrotron  
Radiation, Hermann-von-Helmholtz Platz 1, D-76344 Eggenstein-Leopoldshafen,  
Germany.

\* Correspondence: [andreas.voegelin@eawag.ch](mailto:andreas.voegelin@eawag.ch)

--- 42 pages, 13 tables, 21 figures ---

## Contents

1	Experimental treatments and analytical methods .....	3
2	Formation and aging of Fe(III)- and Ca-precipitates.....	6
3	X-ray diffraction.....	14
4	Fourier-transform infrared spectroscopy (FTIR).....	19
5	X-ray absorption spectroscopy .....	21
6	Kinetic model for Fe(III)-phase fractions and solid-phase P/Fe .....	27
7	Transmission electron microscopy .....	31
7.1	Secondary electron and high-angle annular dark field images.....	31
7.2	STEM-EDX results .....	35
8	Calculation of saturation indices for Ca-phosphates and calcite.....	39
9	References .....	42

# 1 Experimental treatments and analytical methods

**Table S1.** Overview over experimental treatments (background electrolytes, P/Fe ratios, aging times) and analytical techniques for solution analysis and solid characterization <sup>a</sup>.

Electrolyte <sup>b</sup>	(P/Fe) <sub>init</sub> (with Fe = 0.5 mM)				
	0.05 <sup>c</sup>		0.30 <sup>c</sup>		
	Fresh	Aged 100 d	Fresh	Aged 49 d	Aged 100 d
<b>Na</b>	IKFSX	IKFSX	IKFSX	IKFSX	IKFSX
<b>Ca</b>	IKFSX	IKFSX	IKFSX	IKFSX	IKFSX
<b>midCa</b>	IKFX	IKFX	IKFX	IKFX	IKFX
<b>lowCa</b>	IKFX	IKFX	IKFX	IKFX	IKFX
<b>Mg</b>	IKFSX	IKFSX	IKFSX	IKFSX	IKFSX
<b>midMg</b>	IKFX	IKFX	IKFX	IKFX	IKFX
<b>lowMg</b>	IKFX	IKFX	IKFX	IKFX	IKFX
<b>Na+Si</b>	IKFSX	IKFX	IKFSX	IKFSX	IKFSX
<b>Ca+Si</b>	IKFSX	IKFX	IKFSX	IKFSX	IKFSX
<b>Mg+Si</b>	IKFSX	IKFX	IKFSX	IKFSX	IKFSX

<sup>a</sup> For each of the experimental combinations, the initial and final suspensions were analyzed by ICP-MS (I) (initial unfiltered/ filtered with regular sampling intervals). The corresponding precipitates were characterized by Fe K-edge EXAFS (K) spectroscopy, Fourier-transform infrared spectroscopy (FTIR) (F), and X-ray diffraction (XRD) (X). Selected precipitates were also studied with STEM-EDX (S).

<sup>b</sup> Nominal concentrations: *Na*: 8 mM NaHCO<sub>3</sub>; *Ca*: 4 mM CaCO<sub>3</sub>; *midCa*: 1.2 mM CaCO<sub>3</sub> + 5.6 mM NaHCO<sub>3</sub>; *lowCa*: 0.4 mM CaCO<sub>3</sub> + 7.2 mM NaHCO<sub>3</sub>, *Mg*: 4 mM MgO; *midMg*: 1.2 mM MgO + 5.6 mM NaHCO<sub>3</sub>; *lowMg*: 0.4 mM MgO + 7.2 mM NaHCO<sub>3</sub>; *Na+Si*: 8 mM NaHCO<sub>3</sub> + 0.5 mM Na<sub>2</sub>SiO<sub>3</sub>, *Ca+Si*: 4 mM CaCO<sub>3</sub> + 0.5 mM Na<sub>2</sub>SiO<sub>3</sub>, *Mg+Si*: 4 mM MgO + 0.5 mM Na<sub>2</sub>SiO<sub>3</sub>.

<sup>c</sup> Nominal molar P/Fe ratio in the initial solution.

**Table S2.** Total concentrations of Na, Mg, Ca, Fe, Si, P, As, and Cd in experiments at  $(P/Fe)_{init}$  0.30.

Experimental name	Aging t (d)	Electrolyte	$(P/Fe)_{init}$	Na	Mg	Ca	Fe	Si	P	As	Cd
				mM	mM	mM	mM	mM	mM	uM	uM
E06	49	Na	0.29	7.79	-	-	0.48	-	0.15	1.92	1.94
	49	Mg	0.29	-	3.82	-	0.49	-	0.15	1.94	1.96
	49	midMg	0.28	5.45	1.15	-	0.51	-	0.15	1.93	1.94
	49	lowMg	0.30	6.98	0.39	-	0.47	-	0.14	1.90	1.95
	49	Ca	0.31	-	-	3.72	0.47	-	0.15	1.92	1.94
	49	midCa	0.33	5.44	-	1.13	0.46	-	0.15	1.92	1.96
	49	lowCa	0.30	7.12	-	0.39	0.49	-	0.15	1.94	1.99
	54	Na+Si	0.31	8.71	-	-	0.48	0.45	0.15	1.87	1.96
	54	Mg+Si	0.31	-	3.67	-	0.49	0.45	0.15	1.93	1.75
	54	Ca+Si	0.32	-	-	3.76	0.48	0.44	0.15	1.92	1.96
E11	100	Ca	0.31	0.14	-	3.84	0.48	-	0.15	1.95	1.70
	100	midCa	0.30	5.70	-	1.13	0.47	-	0.14	1.93	1.69
	100	lowCa	0.30	7.42	-	0.39	0.48	-	0.15	1.96	1.74
	100	Ca+Si	0.31	-	-	3.82	0.47	0.48	0.14	1.96	1.73
E14	100	Na	0.28	8.06	-	-	0.50	-	0.15	1.97	1.65
	100	Mg	0.30	-	3.68	-	0.50	-	0.15	1.96	1.64
	100	midMg	0.28	5.73	1.15	-	0.49	0.00	0.14	1.96	1.63
	100	lowMg	0.28	7.45	0.36	-	0.49	0.00	0.14	1.96	1.67
	100	Na+Si	0.31	9.17	-	-	0.48	0.49	0.15	2.02	1.73
	100	Mg+Si	0.33	1.24	3.74	-	0.44	0.50	0.15	2.01	1.68

**Table S3.** Total concentrations of Na, Mg, Ca, Fe, Si, P, As, and Cd in experiment at  $(P/Fe)_{init}$  0.05.

Experimental name	Aging t (d)	Electrolyte	$(P/Fe)_{init}$	Na	Mg	Ca	Fe	Si	P	As	Cd
				mM	mM	mM	mM	mM	mM	uM	uM
E10	100	Na	0.044	8.04	-	-	0.49	-	0.025	1.96	1.65
	100	Mg	0.047	-	3.77	-	0.50	-	0.025	1.95	1.63
	100	midMg	0.045	5.63	1.15	-	0.49	-	0.024	1.92	1.61
	100	lowMg	0.045	7.05	0.37	-	0.48	-	0.024	1.91	1.59
	100	Ca	0.049	-	-	4.00	0.49	-	0.025	1.95	1.63
	100	midCa	0.049	5.54	-	1.13	0.48	-	0.025	1.94	1.62
	100	lowCa	0.047	7.15	-	0.40	0.50	-	0.026	1.98	1.67
	100	Na+Si	0.052	9.26	-	-	0.50	0.50	0.026	2.04	1.71
	100	Mg+Si	0.052	-	3.67	-	0.50	0.51	0.025	1.99	1.68
	100	Ca+Si	0.056	-	-	3.90	0.50	0.50	0.026	2.01	1.68

## 2 Formation and aging of Fe(III)- and Ca-precipitates

**Table S4.** Molar ratios of P/Fe, (Ca or Mg)/Fe, and Si/Fe in precipitates formed at  $(P/Fe)_{init}$  0.30 as calculated from ICP-MS solution data (initial total and final filtered concentrations) and as determined by acid digestion of the precipitates obtained by solution filtration.

Electrolyte	Time (d)	ICP-MS solution			Acid digestion		
		(P/Fe) <sub>ppt</sub>	((Ca,Mg)/Fe) <sub>ppt</sub>	Si/Fe	(P/Fe) <sub>ppt</sub>	((Ca,Mg)/Fe) <sub>ppt</sub>	Si/Fe
<b>Na</b>	0	0.29	-	-	0.28	-	-
	3	0.20	-	-	0.19	-	-
	14	0.12	-	-	0.11	-	-
	35	0.08	-	-	0.08	-	-
	49	0.08	-	-	-	-	-
	100	0.07	-	-	0.05	-	-
<b>lowMg</b>	0	0.30	0.09	-	0.29	0.06	-
	3	0.25	0.09	-	0.24	0.08	-
	14	0.18	0.10	-	0.17	0.07	-
	35	0.13	0.09	-	0.12	0.05	-
	49	0.13	0.09	-	-	-	-
	100	0.09	0.05	-	0.09	0.04	-
<b>midMg</b>	0	0.28	0.20	-	0.29	0.07	-
	3	0.24	0.25	-	0.24	0.09	-
	14	0.19	0.23	-	0.19	0.09	-
	35	0.15	0.12	-	0.15	0.07	-
	49	0.13	0.24	-	-	-	-
	100	0.12	0.07	-	0.12	0.06	-
<b>Mg</b>	0	0.29	0.75	-	0.29	0.10	-
	3	0.26	0.54	-	0.26	0.12	-
	14	0.22	0.70	-	0.21	0.11	-
	35	0.18	0.30	-	0.17	0.09	-
	49	0.16	0.56	-	-	-	-
	100	0.16	-0.12*	-	0.14	0.09	-

**Table S4.** Continued.

Electrolyte	Time (d)	ICP-MS solution			Acid digestion		
		(P/Fe) <sub>ppt</sub>	((Ca,Mg)/Fe) <sub>ppt</sub>	Si/Fe	(P/Fe) <sub>ppt</sub>	((Ca,Mg)/Fe) <sub>ppt</sub>	Si/Fe
<b>lowCa</b>	0	0.30	0.16	-	0.29	0.12	-
	3	0.26	0.20	-	0.25	0.14	-
	14	0.20	0.17	-	0.19	0.13	-
	35	0.15	0.14	-	0.14	0.10	-
	49	0.11	0.14	-	0.13	0.10	-
	100	0.11	0.09	-	0.09	0.06	-
<b>midCa</b>	0	0.33	0.40	-	0.30	0.41	-
	3	0.30	0.40	-	0.26	0.22	-
	14	0.25	0.33	-	0.22	0.22	-
	35	0.21	0.30	-	0.18	0.21	-
	49	0.19	0.38	-	0.18	0.21	-
	100	0.15	0.11	-	0.14	0.11	-
<b>Ca</b>	0	0.31	0.92	-	0.30	0.41	-
	3	0.29	0.84	-	0.28	0.43	-
	14	0.27	0.75	-	0.25	0.41	-
	35	0.25	0.58	-	0.22	0.39	-
	49	0.25	0.91	-	0.23	0.24	-
	100	0.27	1.00	-	0.16	0.22	-
<b>Na+Si</b>	0	0.31	-	0.07	0.31	-	0.05
	3	0.29	-	0.08	0.29	-	0.10
	14	0.27	-	0.14	0.26	-	0.10
	35	0.24	-	0.14	0.24	-	0.13
	54	0.23	-	0.13	-	-	-
	100	0.23	-	0.13	0.20	-	0.17
<b>Mg+Si</b>	0	0.31	0.77	0.04	0.32	0.08	0.06
	3	0.30	0.64	0.07	0.31	0.13	0.10
	14	0.29	0.64	0.07	0.29	0.13	0.10
	35	0.28	0.89	0.10	0.27	0.14	0.12
	54	0.27	0.64	0.08	-	-	-
	100	0.27	0.16	0.12	0.25	0.14	0.16
<b>Ca+Si</b>	0	0.32	0.81	0.06	0.33	0.18	0.06
	3	0.32	1.38	0.08	0.31	0.61	0.10
	14	0.31	1.80	0.08	0.30	0.49	0.10
	35	0.31	2.53	0.09	0.30	1.56	0.12
	54	0.31	2.81	0.08	0.30	1.61	0.13
	100	0.29	2.89	0.14	0.27	0.66	0.17

**Table S5.** Molar ratios of P/Fe, (Ca or Mg)/Fe, and Si/Fe in precipitates formed at  $(P/Fe)_{init}$  0.05 as calculated from ICP-MS solution data (initial total and final filtered concentrations) and as determined by acid digestion of the precipitates obtained by solution filtration.

Electrolyte	Time (d)	ICP-MS solution			Acid digestion		
		$(P/Fe)_{ppt}$	$((Ca,Mg)/Fe)_{ppt}$	Si/Fe	$(P/Fe)_{ppt}$	$((Ca,Mg)/Fe)_{ppt}$	Si/Fe
<b>Na</b>	0	0.044	-	-	-	-	-
	1	0.034	-	-	0.032	-	-
	3	0.030	-	-	0.026	-	-
	21	0.026	-	-	0.020	-	-
	70	0.020	-	-	0.016	-	-
	100	0.020	-	-	-	-	-
<b>lowMg</b>	0	0.045	-0.02*	-	-	-	-
	1	0.040	-0.03*	-	0.036	0.011	-
	3	0.036	0.04	-	0.031	0.012	-
	21	0.032	0.05	-	0.027	0.014	-
	70	0.028	0.04	-	0.024	0.015	-
	100	0.027	0.06	-	-	-	-
<b>midMg</b>	0	0.045	0.03	-	-	-	-
	1	0.040	0.00	-	0.038	0.016	-
	3	0.037	0.16	-	0.033	0.016	-
	21	0.034	0.30	-	0.029	0.018	-
	70	0.029	0.09	-	0.026	0.019	-
	100	0.030	0.24	-	-	-	-
<b>Mg</b>	0	0.047	-0.01*	-	-	-	-
	1	0.041	-0.17*	-	0.038	0.025	-
	3	0.038	0.67	-	0.034	0.025	-
	21	0.036	0.70	-	0.030	0.025	-
	70	0.033	0.13	-	0.029	0.027	-
	100	0.033	0.38	-	-	-	-

**Table S5.** Continued.

Electrolyte	Time (d)	ICP-MS solution			Acid digestion		
		(P/Fe) <sub>ppt</sub>	((Ca,Mg)/Fe) <sub>ppt</sub>	Si/Fe	(P/Fe) <sub>ppt</sub>	((Ca,Mg)/Fe) <sub>ppt</sub>	Si/Fe
<b>lowCa</b>	0	0.047	0.02	-	-	-	-
	1	0.041	0.03	-	0.039	0.025	-
	3	0.039	0.08	-	0.033	0.020	-
	21	0.035	0.09	-	0.028	0.022	-
	70	0.030	0.02	-	0.025	0.020	-
	100	0.029	0.06	-	-	-	-
<b>midCa</b>	0	0.049	0.01	-	-	-	-
	1	0.044	0.04	-	0.040	0.027	-
	3	0.040	0.21	-	0.035	0.028	-
	21	0.037	0.16	-	0.030	0.035	-
	70	0.040	0.81	-	0.026	0.061	-
	100	0.042	1.25	-	-	-	-
<b>Ca</b>	0	0.049	-0.20*	-	-	-	-
	1	0.044	-0.24*	-	0.042	0.093	-
	3	0.044	0.94	-	0.039	0.245	-
	21	0.048	2.14	-	0.032	0.300	-
	70	0.049	3.15	-	0.028	0.736	-
	100	0.050	4.07	-	0.055	4.276	-
<b>Na+Si</b>	0	0.052	-	0.14	-	-	-
	1	0.051	-	0.15	0.048	-	0.123
	3	0.051	-	0.27	0.048	-	0.129
	21	0.051	-	0.37	0.046	-	0.158
	70	0.050	-	0.28	0.045	-	0.173
	100	0.050	-	0.32	-	-	-
<b>Mg+Si</b>	0	0.052	-0.19*	0.11	-	-	-
	1	0.051	-0.21*	0.13	0.047	0.041	0.124
	3	0.051	0.49	0.25	0.046	0.043	0.129
	21	0.051	0.59	0.30	0.046	0.050	0.152
	70	0.051	0.30	0.22	0.045	0.063	0.166
	100	0.050	0.66	0.26	-	-	-
<b>Ca+Si</b>	0	0.056	0.89	0.29	-	-	-
	1	0.053	0.02	0.16	0.048	0.219	0.129
	3	0.052	1.52	0.28	0.047	0.517	0.133
	21	0.052	3.08	0.27	0.046	0.596	0.157
	70	0.052	4.02	0.28	0.046	1.283	0.182
	100	0.051	4.65	0.34	0.050	2.953	0.210

**Table S6.** Initial and final concentrations of dissolved Ca and total concentration of PO<sub>4</sub> in the Ca 0.30, Ca+Si 0.30, Ca 0.05 and Ca+Si 0.05 electrolytes. The initial concentration was calculated as the average of the concentration measured right after Fe(II) oxidation and after raising the pH to 7.9, the final concentration was calculated as the average of the concentrations measured after 86 and 100 d of aging.

<b>Experiment</b>	<b>Treatment</b>	<b>Ca(ini)</b>	<b>Ca(end)</b>	<b>P(tot)</b>
		(mM)	(mM)	(mM)
E11	Ca 0.30	3.685	3.417	0.149
E11	Ca+Si 0.30	3.688	2.521	0.140
E10	Ca 0.05	4.003	1.977	0.025
E10	Ca+Si 0.05	3.719	1.663	0.026

For the Ca+Si 0.30, Ca 0.05 and Ca+Si 0.05 treatments, the fraction of PO<sub>4</sub> associated with calcite was calculated from the decrease in the Ca concentration, the STEM-EDX-derived P/Ca ratio of the calcite, and the total PO<sub>4</sub> concentration (see section 4.4.1). For the Ca 0.30 treatment, the fraction of PO<sub>4</sub> associated with Ca-phosphate was calculated by subtracting the dissolved and Fe(III)-precipitate-associated PO<sub>4</sub> from the total PO<sub>4</sub>. Subsequently, the fraction of the Ca precipitated as Ca-phosphate was estimated on the basis of the STEM-EDX-derived P/Ca of amorphous Ca-phosphate and the decrease in Ca during the aging period (see section 4.4.2).

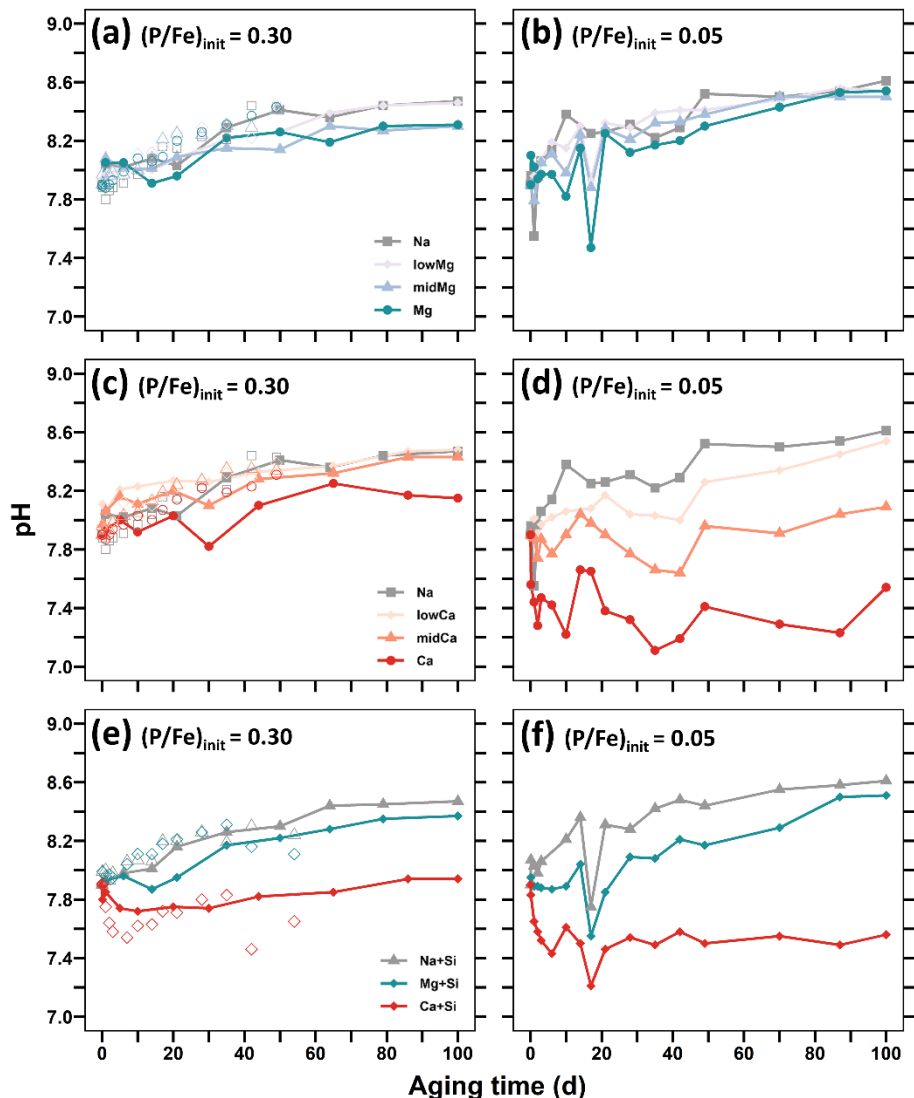


**Figure S1.** pH values of the suspensions (a, b, c) at  $(P/Fe)_{init}$  0.30 and (d, e, f) at  $(P/Fe)_{init}$  0.05. Open symbols in (a, c, e) are values from replicate experiment E06.

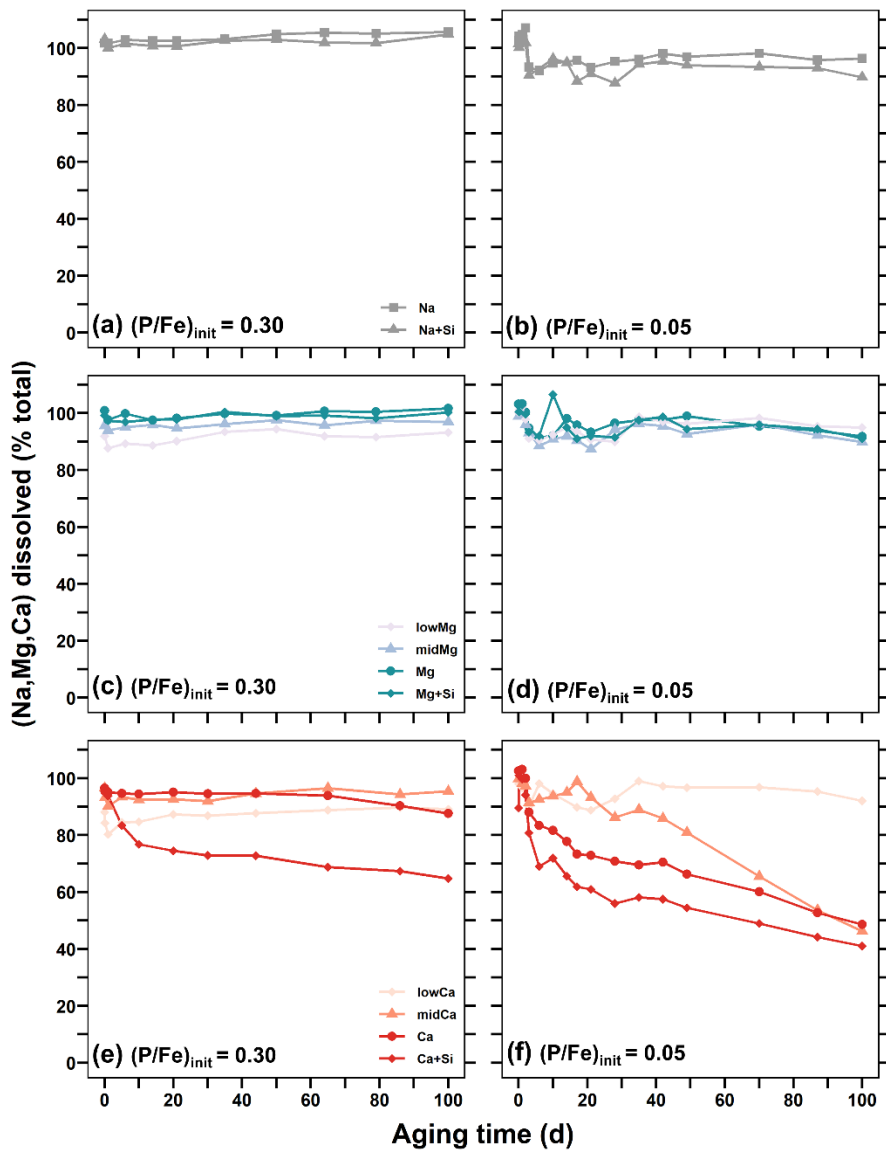


**Figure S2.** Dissolved Na (a, b), Mg (c, d), or Ca (e, f) (% total) in suspensions (a, c, e) at (P/Fe)<sub>init</sub> 0.30 and (b, d, f) at (P/Fe)<sub>init</sub> 0.05.

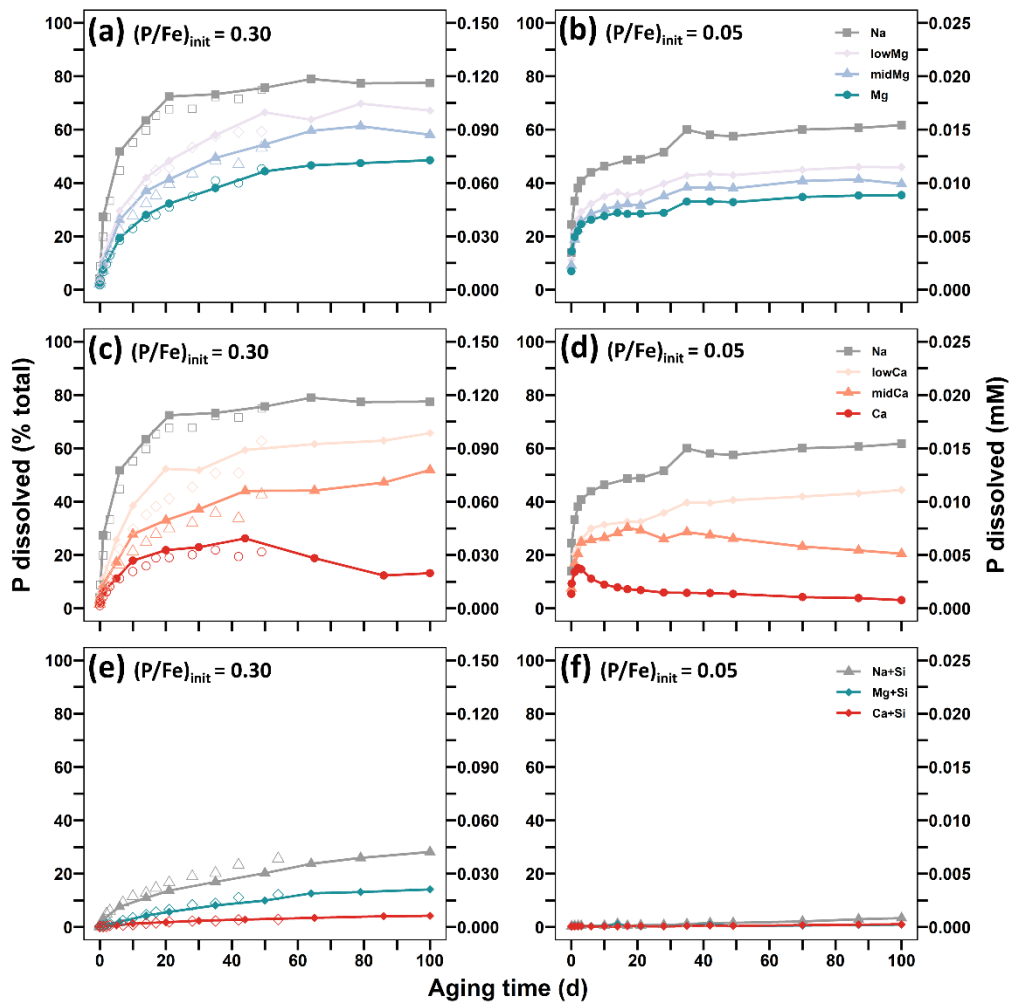


**Figure S3.** Dissolved  $\text{PO}_4$  (% total) in suspensions with replicates (a, c, e) at  $(\text{P}/\text{Fe})_{\text{init}}$  0.30 and (b, d, f) at  $(\text{P}/\text{Fe})_{\text{init}}$  0.05. Open shapes in (a, c, e) are the replicates from experiment E06.

### 3 X-ray diffraction

For XRD analysis, 10 mg of dried precipitate were suspended in ethanol, transferred onto 27-mm diameter low-background Si-slides and allowed to dry. XRD patterns were recorded from 10 to 90 or 5 to 95° 2-θ with a step-size of 0.017° and a measurement time of 2.5 or 7 h per sample using Co K $\alpha$  radiation (X'Pert Powder diffractometer with XCelerator detector, PANalytical, Almelo, The Netherlands).

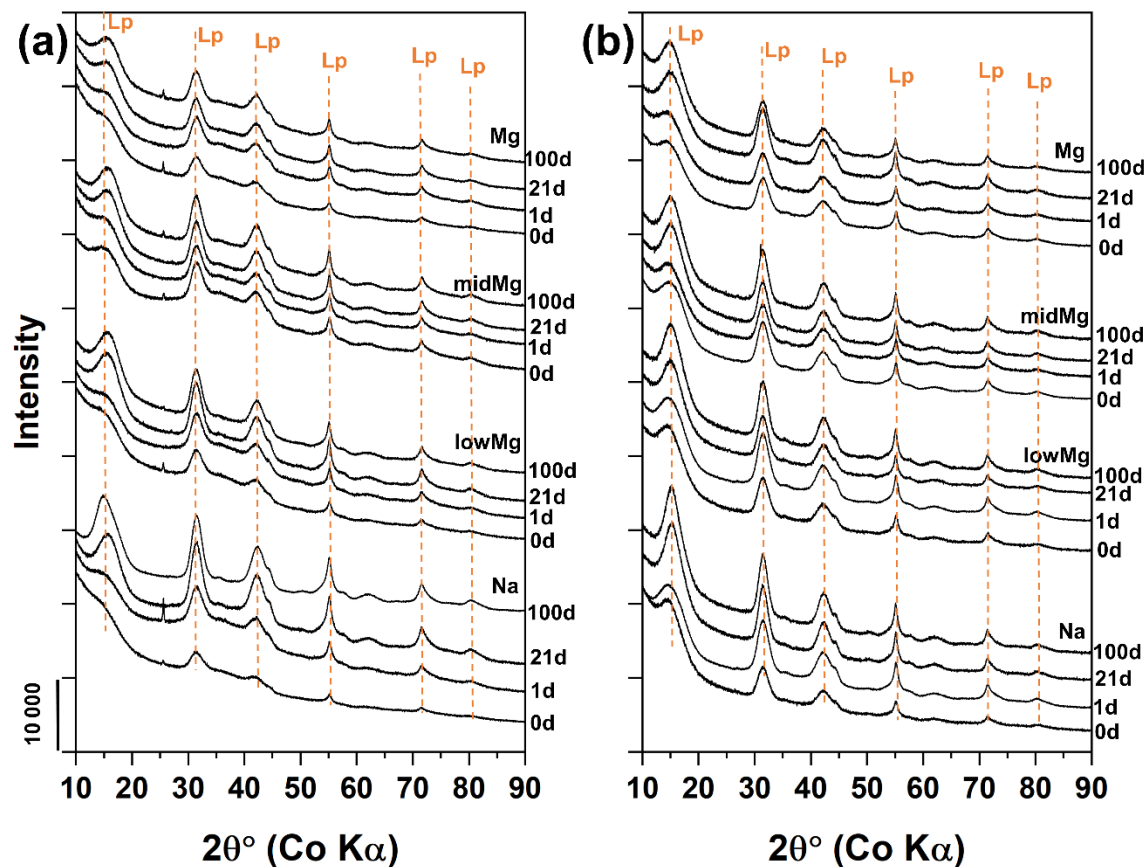


**Figure S4.** X-ray diffraction patterns of Fe(III)-precipitates formed and aged in Na- and Mg-background electrolytes. (a) Precipitates formed and aged at  $(P/Fe)_{init}$  0.30. (b) Precipitates formed and aged at  $(P/Fe)_{init}$  0.05.

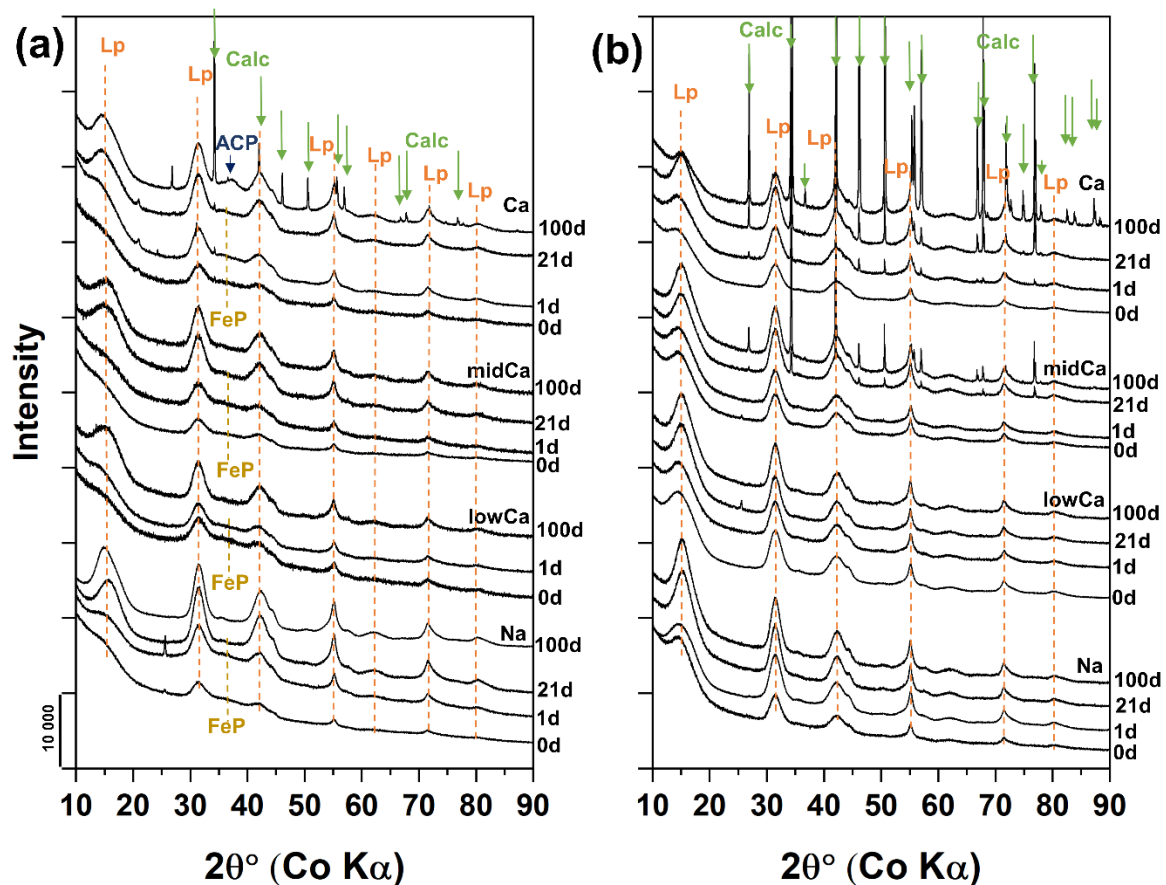


**Figure S5.** X-ray diffraction patterns of Fe-, and Ca-precipitates formed and aged in Na- and Ca-background electrolytes. (a) Precipitates formed and aged at  $(P/Fe)_{init}$  0.30. (b) Precipitates formed and aged at  $(P/Fe)_{init}$  0.05.

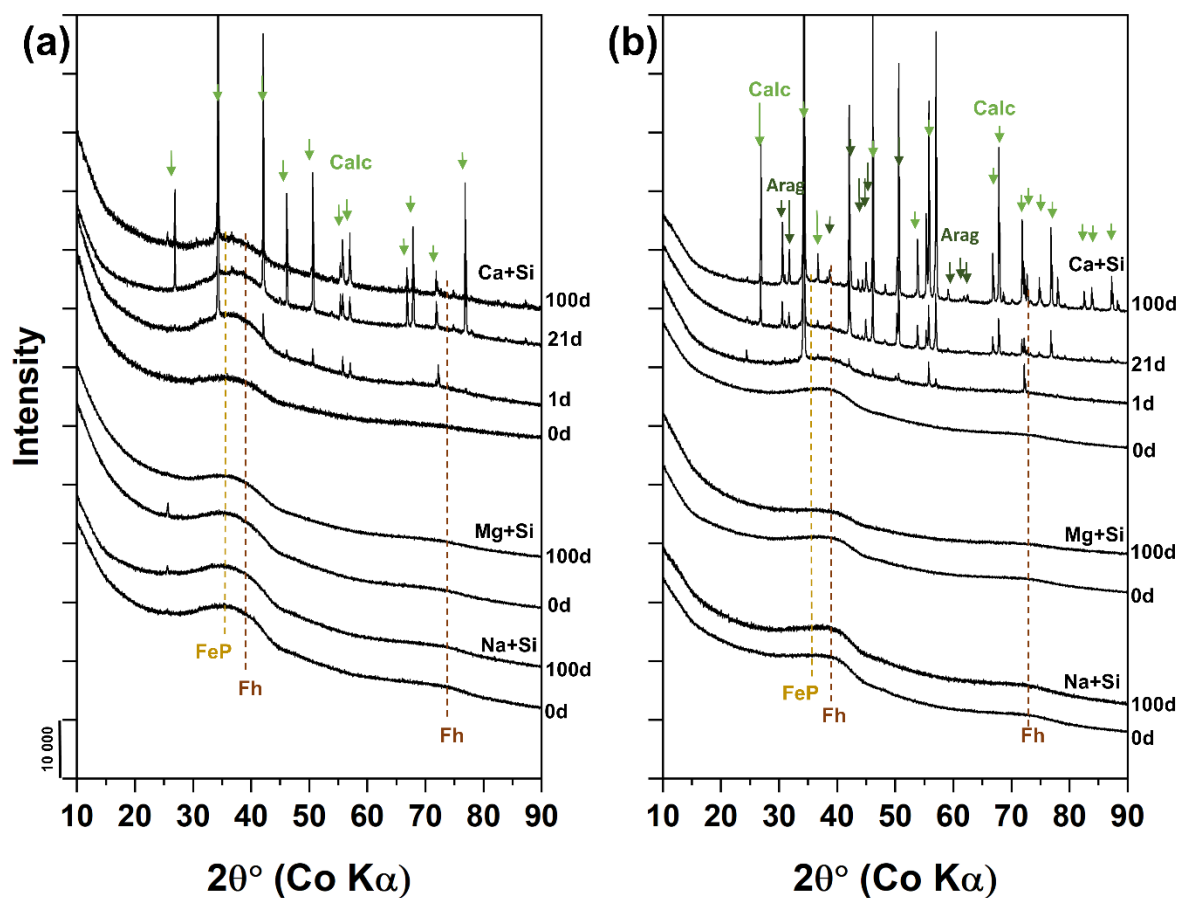


**Figure S6.** X-ray diffraction patterns of Fe-, and Ca-precipitates formed and aged in background electrolytes containing 0.5 mM Si. (a) Precipitates formed and aged at  $(P/Fe)_{init}$  0.30. (b) Precipitates formed and aged at  $(P/Fe)_{init}$  0.05.

**Table S7.** Full width at half maxima (FWHM) of the 020 peak of lepidocrocite (Lp) and corresponding coherently scattering domain sizes (L) estimated with Scherrer equation (shape factor K = 0.9,  $\lambda$  = 1.79 Å (Co K $\alpha$ ), peak position at 15.97° 2 $\theta$ ) for precipitates formed at (P/Fe)<sub>init</sub> of 0.30 and 0.05 in Na, Mg and Ca electrolytes.

Treatment	Time (d)	FWHM (°)	L (nm)
<b>Na 0.30</b>	0	9.24	1.01
	1	8.37	1.11
	21	6.03	1.55
	49	5.41	1.72
	100	5.18	1.80
<b>Mg 0.30</b>	0	13.26	0.70
	1	10.09	0.92
	21	6.87	1.36
	49	6.52	1.43
	100	5.88	1.59
<b>Ca 0.30</b>	0	11.22	0.83
	1	9.78	0.95
	49	6.03	1.47
	100	5.52	1.67
Treatment	Time (d)	FWHM (°)	L (nm)
<b>Na 0.05</b>	0	5.87	1.58
	6	4.68	1.99
	49	4.10	2.27
	100	3.77	2.47
<b>Mg 0.05</b>	0	6.77	1.38
	6	6.57	1.42
	49	5.37	1.74
	100	5.24	1.78
<b>Ca 0.05</b>	0	6.51	1.43
	6	5.38	1.73
	49	4.40	2.12
	100	4.64	2.01

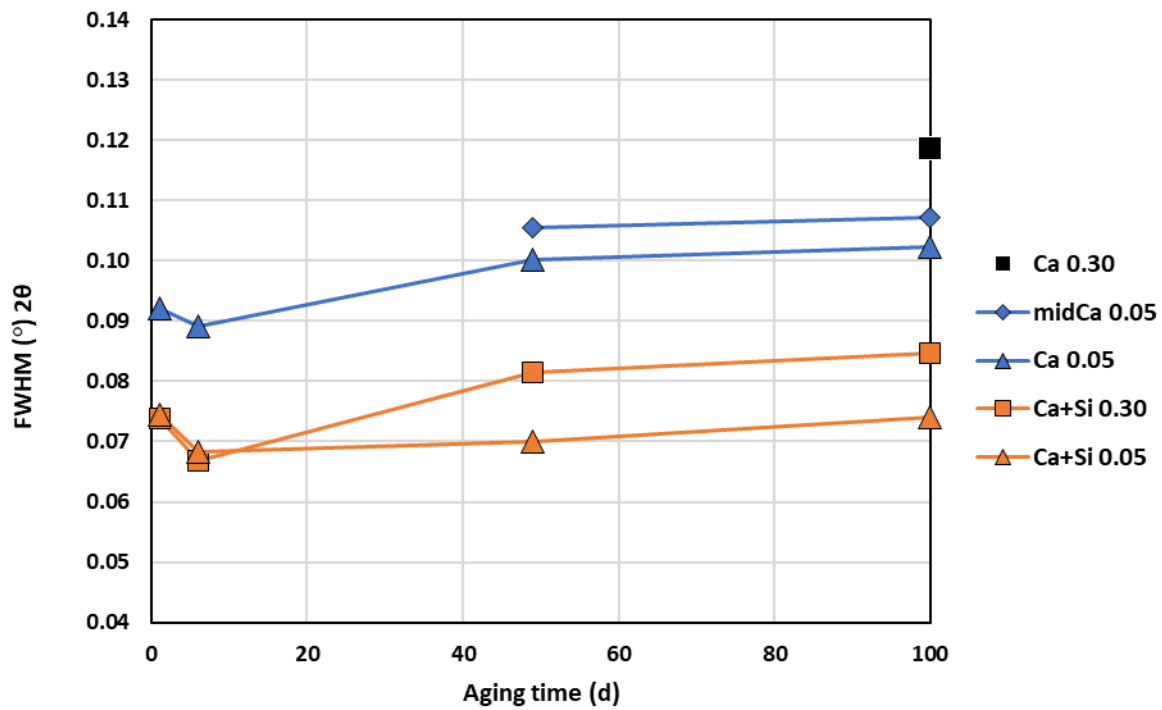


**Figure S7.** Full width at half maximum (FWHM) of the calcite peak at  $34.30^\circ 2\theta$ .

## 4 Fourier-transform infrared spectroscopy (FTIR)

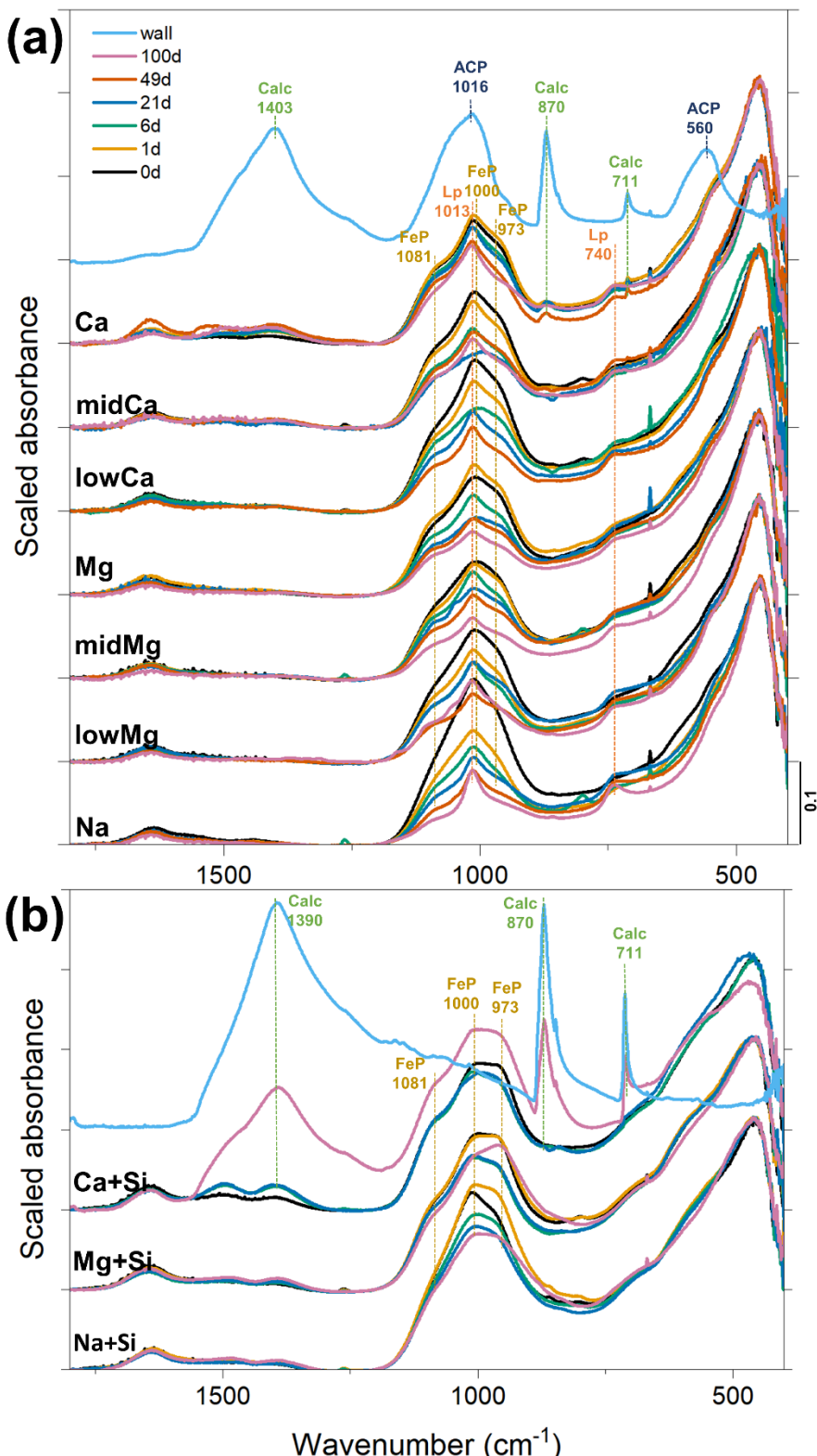


**Figure S8.** FTIR spectra of precipitates formed and aged up to 100 d at  $(\text{P}/\text{Fe})_{\text{init}} 0.30$  in Na, low Mg, midMg, Mg, lowCa and Ca electrolytes (a) and Ca+Si, Mg+Si, and Na+Si electrolytes (b). Spectra with the label “wall” were collected on precipitates scraped off from the walls of the reaction vessel at the last sampling point (100 d) in the Ca and Ca+Si electrolytes.

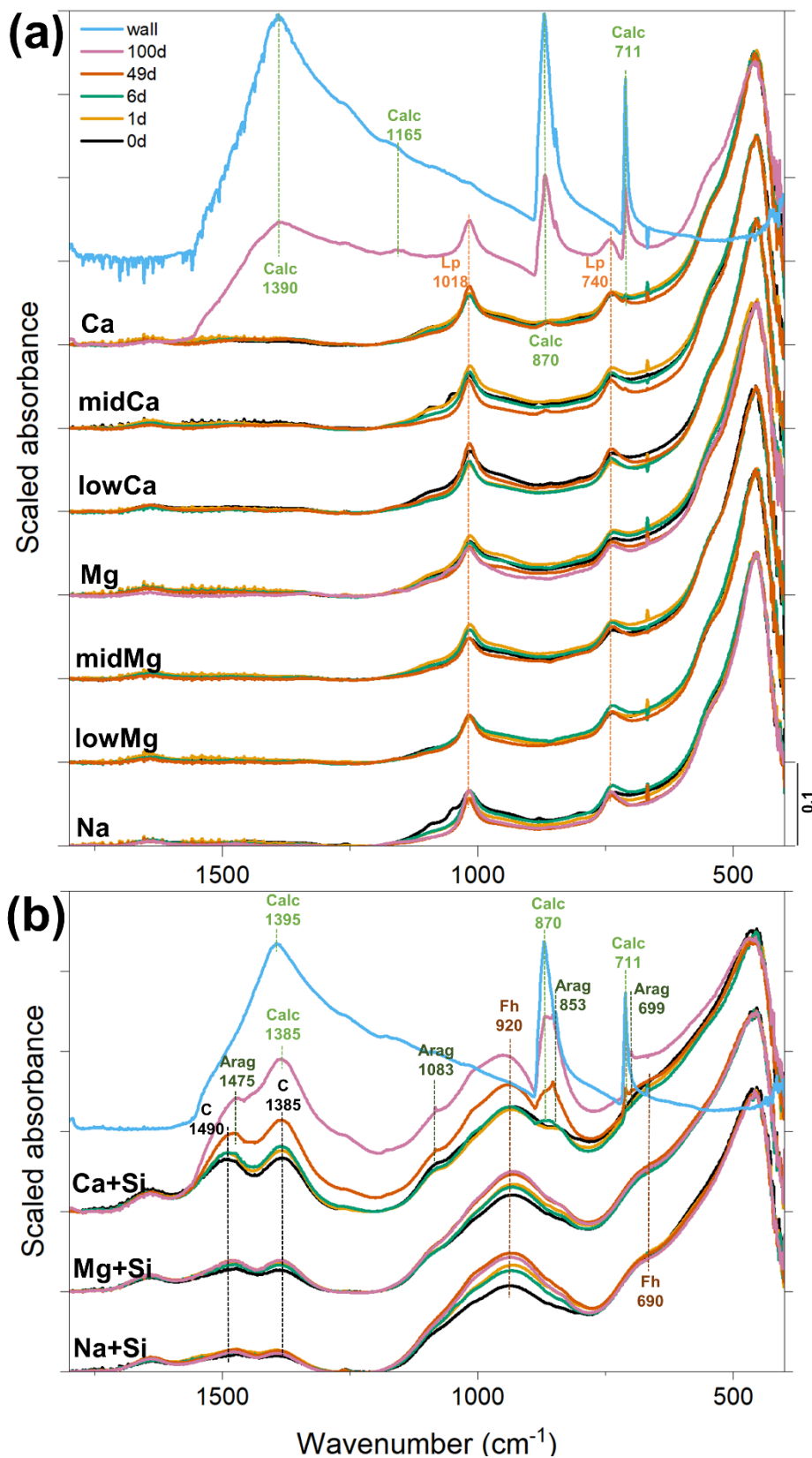


**Figure S9.** FTIR spectra of precipitates formed and aged up to 100 d at  $(\text{P}/\text{Fe})_{\text{init}} 0.05$  in Na, low Mg, midMg, Mg, lowCa, midCa and Ca electrolytes (a) and Ca+Si, Mg+Si, and Na+Si electrolytes (b). Spectra with the label “wall” were collected on precipitates scraped off from the walls of the reaction vessel at the last sampling point (100 d) in the Ca and Ca+Si electrolytes.

## 5 X-ray absorption spectroscopy

**Table S8.** Fe K-edge EXAFS LCF results for precipitates formed and aged at  $(P/Fe)_{init}$  0.30. The LCF results are presented graphically in Fig. 6. The LCF analysis is described in the section 2.5.

Electrolyte	Time (d)	Lp*	Fh*	FeP*	CaFeP*	sum	rfactor
Na	0	0.28	0.25	0.46	0.00	0.99	0.00040
	1	0.41	0.25	0.33	0.00	0.98	0.00054
	3	0.45	0.30	0.25	0.00	1.00	0.00060
	6	0.55	0.20	0.21	0.00	0.96	0.00122
	14	0.60	0.30	0.06	0.00	0.96	0.00103
	35	0.68	0.26	0.01	0.00	0.95	0.00121
	49	0.65	0.34	0.01	0.00	1.00	0.00055
	50	0.80	0.13	0.04	0.00	0.97	0.00106
	100	0.83	0.10	0.02	0.00	0.96	0.00057
lowMg	0	0.33	0.26	0.40	0.00	1.00	0.00065
	1	0.42	0.22	0.34	0.00	0.98	0.00033
	6	0.51	0.24	0.23	0.00	0.98	0.00076
	35	0.58	0.34	0.07	0.00	1.00	0.00184
	49	0.58	0.41	0.00	0.00	0.99	0.00093
	50	0.61	0.27	0.10	0.00	0.98	0.00179
	100	0.64	0.33	0.01	0.00	0.98	0.00053
midMg	0	0.32	0.34	0.34	0.00	1.00	0.00053
	1	0.42	0.24	0.32	0.00	0.99	0.00049
	6	0.48	0.29	0.22	0.00	0.99	0.00051
	35	0.52	0.39	0.09	0.00	1.00	0.00097
	49	0.52	0.41	0.05	0.01	1.00	0.00062
	50	0.55	0.39	0.06	0.00	1.00	0.00054
	100	0.58	0.38	0.04	0.00	1.00	0.00065
Mg	0	0.33	0.33	0.34	0.00	1.00	0.00045
	1	0.39	0.30	0.31	0.00	1.00	0.00046
	3	0.38	0.35	0.26	0.00	1.00	0.00051
	6	0.43	0.29	0.24	0.01	0.98	0.00131
	14	0.43	0.36	0.13	0.07	1.00	0.00169
	35	0.45	0.46	0.06	0.03	1.00	0.00096
	49	0.45	0.49	0.07	0.00	1.01	0.00072
	50	0.50	0.47	0.03	0.00	1.00	0.00052
	100	0.52	0.45	0.03	0.00	1.00	0.00058

**Table S8.** Continued.

<b>Electrolyte</b>	<b>Time (d)</b>	<b>Lp*</b>	<b>Fh*</b>	<b>FeP*</b>	<b>CaFeP*</b>	<b>sum</b>	<b>rfactor</b>
<b>lowCa</b>	0	0.36	0.28	0.35	0.00	1.00	0.00043
	1	0.47	0.19	0.24	0.08	0.99	0.00046
	6	0.56	0.15	0.18	0.09	0.98	0.00117
	35	0.67	0.26	0.08	0.00	1.00	0.00084
	44	0.65	0.26	0.05	0.00	0.97	0.00070
	49	0.66	0.26	0.08	0.00	1.00	0.00055
	100	0.68	0.27	0.02	0.00	0.97	0.00150
<b>midCa</b>	0	0.38	0.30	0.28	0.04	1.00	0.00031
	1	0.49	0.18	0.16	0.16	0.99	0.00038
	6	0.56	0.24	0.11	0.08	0.99	0.00106
	35	0.63	0.25	0.06	0.05	1.00	0.00096
	44	0.60	0.29	0.10	0.00	0.99	0.00070
	49	0.64	0.19	0.06	0.08	0.96	0.00040
	100	0.64	0.27	0.07	0.00	0.98	0.00056
<b>Ca</b>	0	0.43	0.29	0.16	0.13	1.01	0.00043
	1	0.51	0.20	0.06	0.23	0.99	0.00040
	3	0.50	0.25	0.13	0.12	1.00	0.00032
	6	0.56	0.21	0.04	0.18	1.00	0.00058
	14	0.58	0.18	0.08	0.16	0.99	0.00167
	35	0.63	0.23	0.12	0.02	1.00	0.00090
	44	0.63	0.21	0.14	0.01	0.98	0.00038
	49	0.63	0.18	0.07	0.12	0.99	0.00049
	100	0.73	0.22	0.03	0.00	0.99	0.00050
<b>Na+Si</b>	0	-	0.45	0.49	0.04	0.98	0.00117
	1	-	0.50	0.49	0.00	0.99	0.00056
	7	-	0.53	0.46	0.00	0.99	0.00046
	21	-	0.56	0.43	0.00	0.99	0.00067
	54	-	0.60	0.39	0.00	0.99	0.00046
	100	-	0.62	0.36	0.00	0.98	0.00100
<b>Mg+Si</b>	0	-	0.54	0.45	0.00	0.99	0.00084
	1	-	0.55	0.43	0.00	0.98	0.00076
	7	-	0.56	0.43	0.00	0.99	0.00061
	21	-	0.58	0.41	0.00	0.99	0.00098
	50	-	0.60	0.38	0.00	0.98	0.00070
	54	-	0.61	0.37	0.00	0.98	0.00088
	100	-	0.60	0.38	0.00	0.98	0.00078
<b>Ca+Si</b>	0	-	0.59	0.14	0.26	1.00	0.00046
	1	-	0.61	0.12	0.26	0.99	0.00055
	7	-	0.58	0.12	0.29	0.99	0.00060
	21	-	0.59	0.13	0.28	1.00	0.00201
	44	-	0.58	0.10	0.32	0.99	0.00129
	54	-	0.62	0.20	0.18	0.99	0.00186
	100	-	0.62	0.09	0.29	1.00	0.00144

**Table S9.** Fe K-edge EXAFS LCF results for precipitates formed and aged at  $(P/Fe)_{init}$  0.05. The LCF results are presented graphically in Fig. 6. The LCF analysis is described in the section 2.5.

Electrolyte	Time (d)	Lp*	Fh*	FeP*	sum	rfactor
Na	0	0.793	0.202	-	0.995	0.00078
	1	0.796	0.214	-	1.010	0.00185
	3	0.797	0.215	-	1.012	0.00181
	6	0.870	0.127	-	0.997	0.000524
	21	0.950	0.041	-	0.991	0.000577
	49	0.939	0.047	-	0.986	0.000503
	100	0.996	0.003	-	0.999	0.000489
lowMg	0	0.862	0.124	-	0.986	0.00032
	6	0.861	0.146	-	1.007	0.00039
	21	0.892	0.101	-	0.993	0.00044
	49	0.907	0.072	-	0.979	0.00062
	100	0.949	0.047	-	0.996	0.00028
midMg	0	0.798	0.201	-	0.999	0.00025
	6	0.844	0.154	-	0.997	0.00031
	21	0.868	0.128	-	0.996	0.00046
	49	0.885	0.094	-	0.979	0.00064
	100	0.928	0.071	-	0.999	0.00044
Mg	0	0.748	0.241	-	0.989	0.00177
	1	0.764	0.247	-	1.011	0.00220
	3	0.755	0.256	-	1.011	0.00280
	6	0.802	0.195	-	0.997	0.00050
	21	0.834	0.167	-	1.001	0.00035
	49	0.850	0.142	-	0.992	0.00052
	100	0.884	0.116	-	1.000	0.00081

**Table S9.** Continued.

<b>Electrolyte</b>	<b>Time (d)</b>	<b>Lp*</b>	<b>Fh*</b>	<b>FeP*</b>	<b>sum</b>	<b>rfactor</b>
<b>lowCa</b>	0	0.887	0.105	-	0.993	0.00040
	6	0.909	0.098	-	1.007	0.00037
	21	0.936	0.062	-	0.998	0.00037
	49	0.955	0.026	-	0.981	0.00052
	100	0.992	0.000	-	0.992	0.00034
<b>midCa</b>	0	0.861	0.127	-	0.988	0.00042
	6	0.891	0.104	-	0.995	0.00030
	21	0.924	0.075	-	0.999	0.00059
	49	0.946	0.041	-	0.987	0.00060
	100	1.000	0.000	-	1.000	0.00119
<b>Ca</b>	0	0.803	0.190	-	0.993	0.000586
	1	0.809	0.203	-	1.012	0.002239
	3	0.809	0.221	-	1.029	0.002576
	6	0.867	0.135	-	1.003	0.000708
	21	0.957	0.043	-	1.000	0.000543
	49	0.975	0.007	-	0.982	0.002302
	100	0.984	0.007	-	0.991	0.00809
<b>Na+Si</b>	0	-	0.897	0.087	0.983	0.001121
	1	-	0.868	0.117	0.985	0.002889
	3	-	0.906	0.087	0.994	0.00355
	6	-	0.875	0.114	0.989	0.00028
	21	-	0.851	0.136	0.987	0.000691
	49	-	0.836	0.146	0.982	0.001608
	100	-	0.866	0.124	0.990	0.000671
<b>Mg+Si</b>	0	-	0.873	0.105	0.978	0.0007
	1	-	0.890	0.093	0.983	0.0054
	3	-	0.855	0.129	0.985	0.0039
	6	-	0.875	0.116	0.991	0.0005
	21	-	0.837	0.149	0.987	0.0007
	49	-	0.833	0.148	0.981	0.0012
	100	-	0.851	0.135	0.986	0.0007
<b>Ca+Si</b>	0	-	0.891	0.102	0.993	0.0014
	1	-	0.811	0.183	0.995	0.0041
	3	-	0.814	0.180	0.995	0.0068
	6	-	0.882	0.125	1.007	0.0005
	21	-	0.816	0.180	0.997	0.0023
	49	-	0.848	0.147	0.995	0.0019
	100	-	0.886	0.117	1.003	0.0037

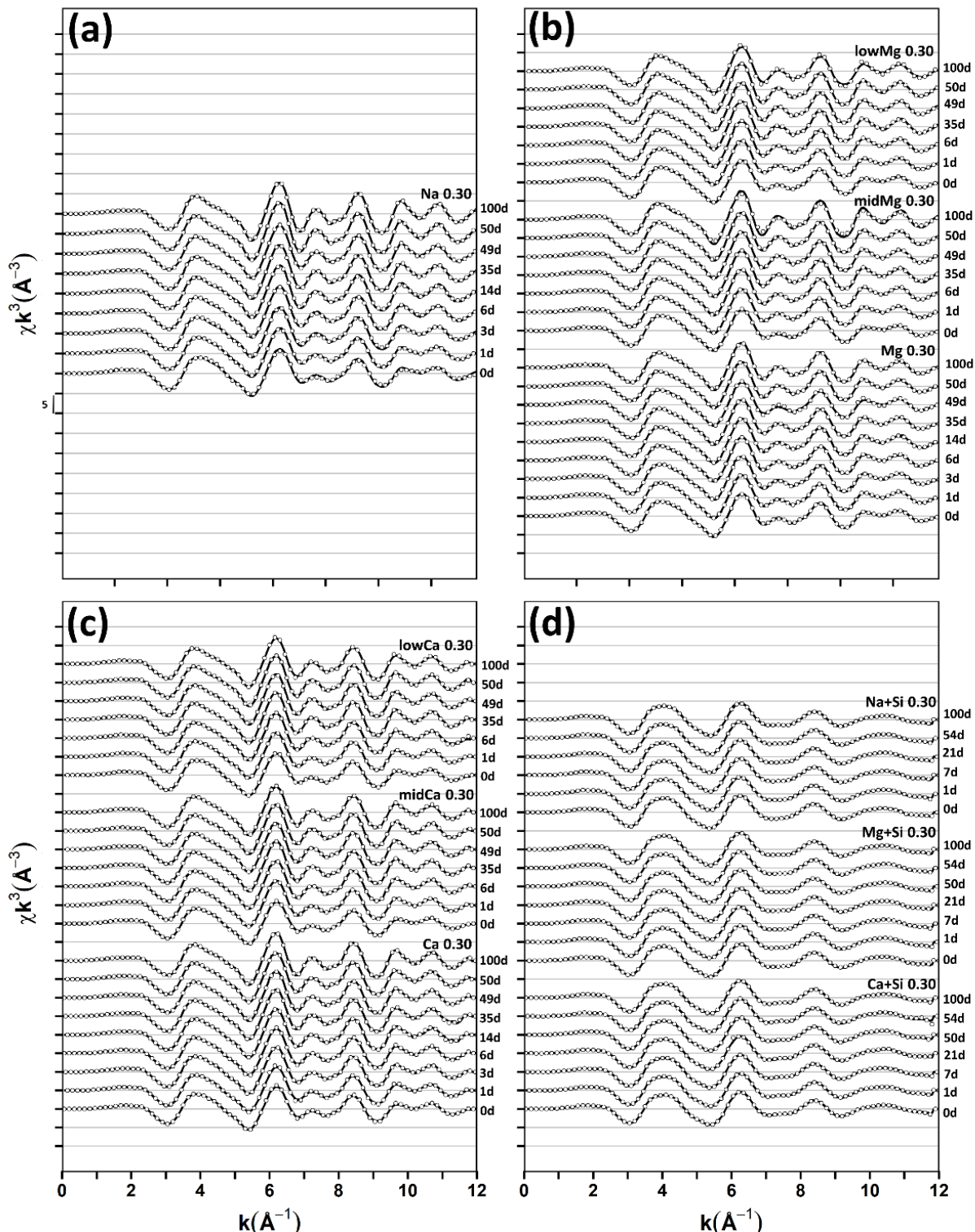


**Figure S10.**  $k^3$ -weighted Fe K-edge EXAFS spectra (solid lines) with reconstructed LCF spectra (open circles). (a) Na 0.30, (b) lowMg 0.30, midMg 0.30, Mg 0.30, (c) lowCa 0.30, midCa 0.30, Ca 0.30, (d) Na+Si 0.30, Mg+Si 0.30, Ca+Si 0.30.

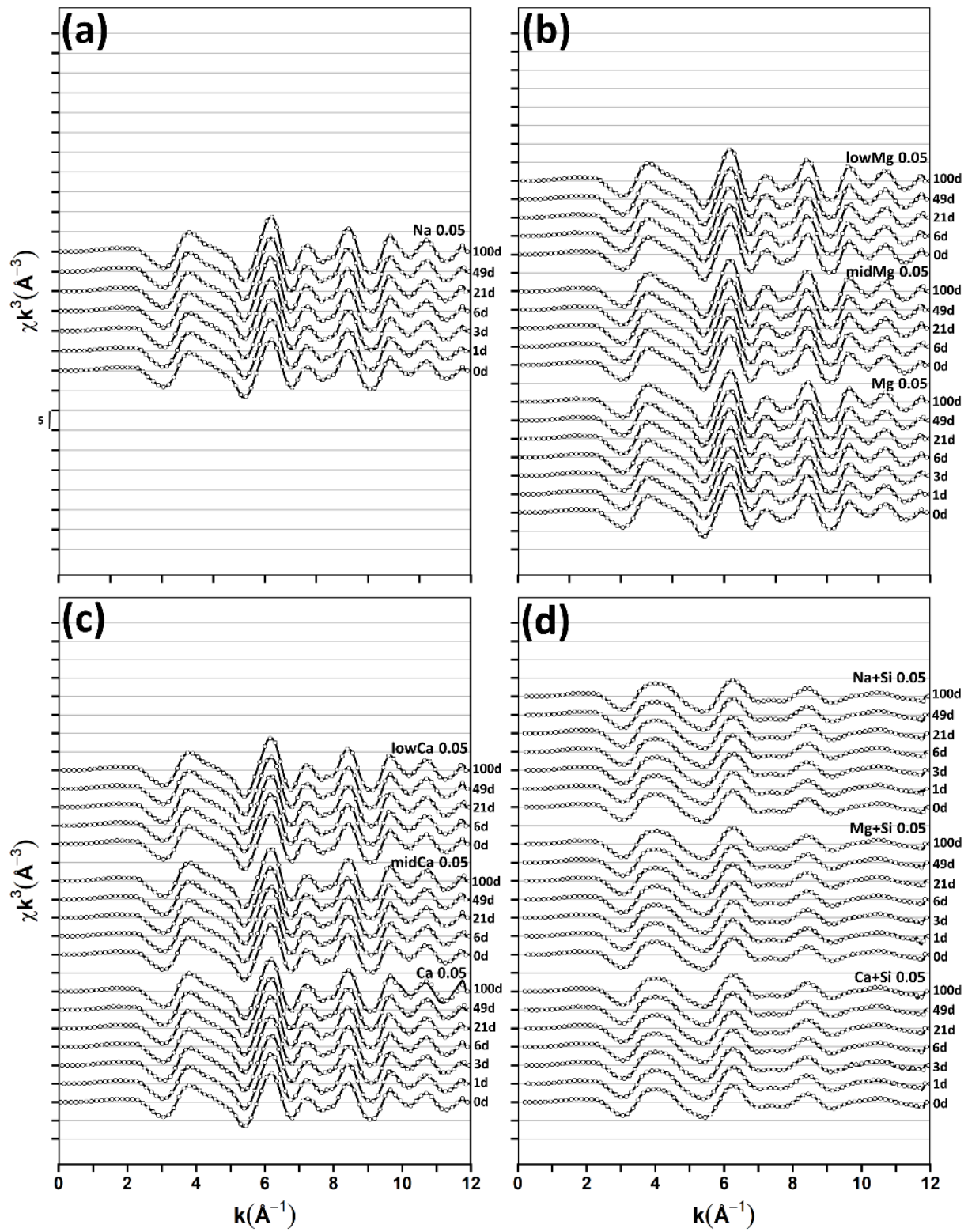


**Figure S11.**  $k^3$ -weighted Fe K-edge EXAFS spectra (solid lines) with reconstructed LCF spectra (open circles). (a) Na 0.05, (b) lowMg 0.05, midMg 0.05, Mg 0.05, (c) lowCa 0.05, midCa 0.05, Ca 0.05, (d) Na+Si 0.05, Mg+Si 0.05, Ca+Si 0.05.

## 6 Kinetic model for Fe(III)-phase fractions and solid-phase P/Fe

A kinetic model was set up to describe the temporal changes in the fractions of different types of Fe(III)-precipitates obtained by Fe K-edge EXAFS analysis (Fig. 6) and to link these fractions with related changes in the molar  $(P/Fe)_{ppt}$  ratios of the bulk precipitates as calculated from changes in dissolved  $PO_4$  over time (Fig. 1). The aim was to derive rate coefficients for the transformations of amorphous into more polymerized or crystalline Fe(III)-solids and the  $(P/Fe)$  ratios of the respective structural units.

For the model calculations, the sum of the LCF-derived normalized fractions of FeP and CaFeP was taken as the fraction of (Ca-)Fe(III)-phosphate, (Ca)FeP. Note that for the LCF analysis of spectra from the treatments at  $(P/Fe)_{init}$  of 0.30, the reference spectra FeP\* and CaFeP\* were used to represent (Ca)FeP, whereas for the spectra from the treatments at  $(P/Fe)_{init}$  of 0.05 with  $SiO_4$ , only the FeP\* reference spectrum was used to represent the minor fractions of (Ca)FeP in these samples. The LCF-derived fraction of Fh\* representing  $PO_4$ -loaded Fh in the  $SiO_4$ -free electrolytes and mostly  $SiO_4$ -loaded Fh in the  $SiO_4$ -containing electrolytes. The LCF-derived fraction for the Lp\* reference spectrum was interpreted as Lp fraction in the precipitates

For the treatments without  $SiO_4$  at  $(P/Fe)_{init}$  of 0.30, where the precipitates contained relevant fractions of (Ca)FeP, Fh and Lp based on the LCF results, the following transformation reactions were considered with first order rate coefficients k:



Thus, it was assumed that (Ca)FeP can transform either into Fh or Lp and that Fh can further transform into Lp following first-order reaction kinetics. We also tested two models that were based on only two transformation reactions: (i) Consecutive model in which (Ca)FeP transforms into Fh and Fh into Lp (R1 and R2). (ii) Parallel model in which (Ca)FeP transforms into Lp, in parallel to Fh transformation into Lp (R2 and R3). The consecutive model predicted a marked initial increase of the Fh fractions that did not match the data. The parallel model performed better, but was not able to describe the increase in Fh during aging of the Mg-containing electrolytes at  $(P/Fe)_{init}$  of 0.30. Thus, the model with all 3 transformation reactions was best suited to describe all 7 experiments at  $(P/Fe)_{init}$  of 0.30 without  $SiO_4$ .

For all other treatments, the model reduced to a single transformation reaction:

For the treatments with  $SiO_4$  at  $(P/Fe)_{init}$  of 0.30 and 0.05, only the transformation reaction of (Ca)FeP into Fh (R1) was included, as no Lp formed in this system. For the treatments without  $SiO_4$  at  $(P/Fe)_{init}$  of 0.05, the kinetic model was limited to the transformation of Fh into Lp (R3), since no (Ca)FeP was detected by the LCF analysis.

The kinetic model was set up in Microsoft Excel® spreadsheets using the solver routine for parameter optimization. In individual spreadsheets for each treatment, the fractions of (Ca)FeP, Fh and Lp were calculated over time-increments of 0.25 d from 0 to 100 days, based on their initial fractions and the first-order rate coefficients as optimizable parameters. Since the sum of the fractions equaled 1, only 2 fractions were refined for the SiO<sub>4</sub>-free electrolytes at (P/Fe)<sub>init</sub> of 0.30, and 1 for all other treatments, and the remaining third or second fraction was calculated by difference. For parameter refinement, the sum of the squared residuals was calculated from all EXAFS-derived phase fractions ((Ca)FeP, Fh, Lp) for each analyzed time point (SSR<sub>fractions</sub>).

By assuming a constant molar (P/Fe) for (Ca)FeP, Fh and Lp in each treatment ((P/Fe)<sub>(Ca)FeP</sub>, (P/Fe)<sub>Fh</sub>, (P/Fe)<sub>Lp</sub>), and using the modelled fractions of (Ca)FeP, Fh and Lp, the bulk (P/Fe)<sub>pp</sub> of the entire precipitate as a function of aging time could be calculated. For the refinement of the parameters (P/Fe)<sub>(Ca)FeP</sub>, (P/Fe)<sub>Fh</sub>, and (P/Fe)<sub>Lp</sub> in each treatment, the sum of squared residuals was calculated from the modelled and experimental (P/Fe)<sub>pp</sub> (SSR<sub>ratios</sub>). In the Ca 0.30 treatment, only experimental (P/Fe)<sub>pp</sub> values up to 20 days of aging were considered, due to the subsequent onset of Ca-phosphate precipitation. For the Ca 0.05 and midCa 0.05 treatments, only the experimental (P/Fe)<sub>pp</sub> values up to day 3 and 6, respectively, were included, due to the subsequent co-precipitation of PO<sub>4</sub> with calcite.

For parameter refinement, all ten treatments with the same (P/Fe)<sub>init</sub> were refined simultaneously using the GRG nonlinear engine of the solver routine, and constraining all parameters to non-negative values. In a first step of parameter refinement, the initial fractions and rate coefficients were optimized, i.e., the EXAFS derived results, by minimizing the SSR<sub>fractions</sub>. As start values, all rates were set to zero, and all precipitate fractions were set to the same value. Based on the refined initial fractions and rate coefficients, the (P/Fe) ratios of the individual structural components were subsequently refined by minimizing the SSR<sub>ratios</sub>. Starting from this first fit, all model parameters, i.e., the initial fractions, rate coefficients, and (P/Fe) ratios of the individual structural components were subsequently refined simultaneously by minimizing the total SSR (TSSR). The TSSR was calculated as the weighted sum of SSR<sub>fractions</sub> and SSR<sub>ratios</sub>. In 3 subsequent fits, the SSR<sub>ratios</sub> was weighed by factors of 10, 20 and 50, thus allocating an increasing importance to the accurate fit of the (P/Fe) ratios. To reduce the number of adjustable parameters and to render the fits more robust, the following constraints were introduced:

For the treatments at (P/Fe)<sub>init</sub> of 0.30 without SiO<sub>4</sub>, the (P/Fe)<sub>Fh</sub> and (P/Fe)<sub>Lp</sub> were set equal for all treatments, whereas the (P/Fe)<sub>(Ca)FeP</sub> were individually refined. Equally, for the SiO<sub>4</sub>-containing treatments at (P/Fe)<sub>init</sub> of 0.30, a common (P/Fe)<sub>Fh</sub> was fit, but individual (P/Fe)<sub>(Ca)FeP</sub> for each electrolyte.

For the fit of all treatments at (P/Fe)<sub>init</sub> of 0.05 without SiO<sub>4</sub>, the (P/Fe)<sub>Lp</sub> were set equal for all electrolytes, whereas the (P/Fe)<sub>Fh</sub> were individually refined for each electrolyte. For the SiO<sub>4</sub>-containing electrolytes at (P/Fe)<sub>init</sub> of 0.05, the rate coefficients k<sub>(Ca)FeP-Fh</sub> were set to 0, as no clear temporal trends were visible in the precipitate fractions (i.e., the refined initial fractions of (Ca)FeP and Fh were assumed to remain constant over time), and the (P/Fe)<sub>Fh</sub> was set to 0 to constrain the results for (P/Fe)<sub>(Ca)FeP</sub>.

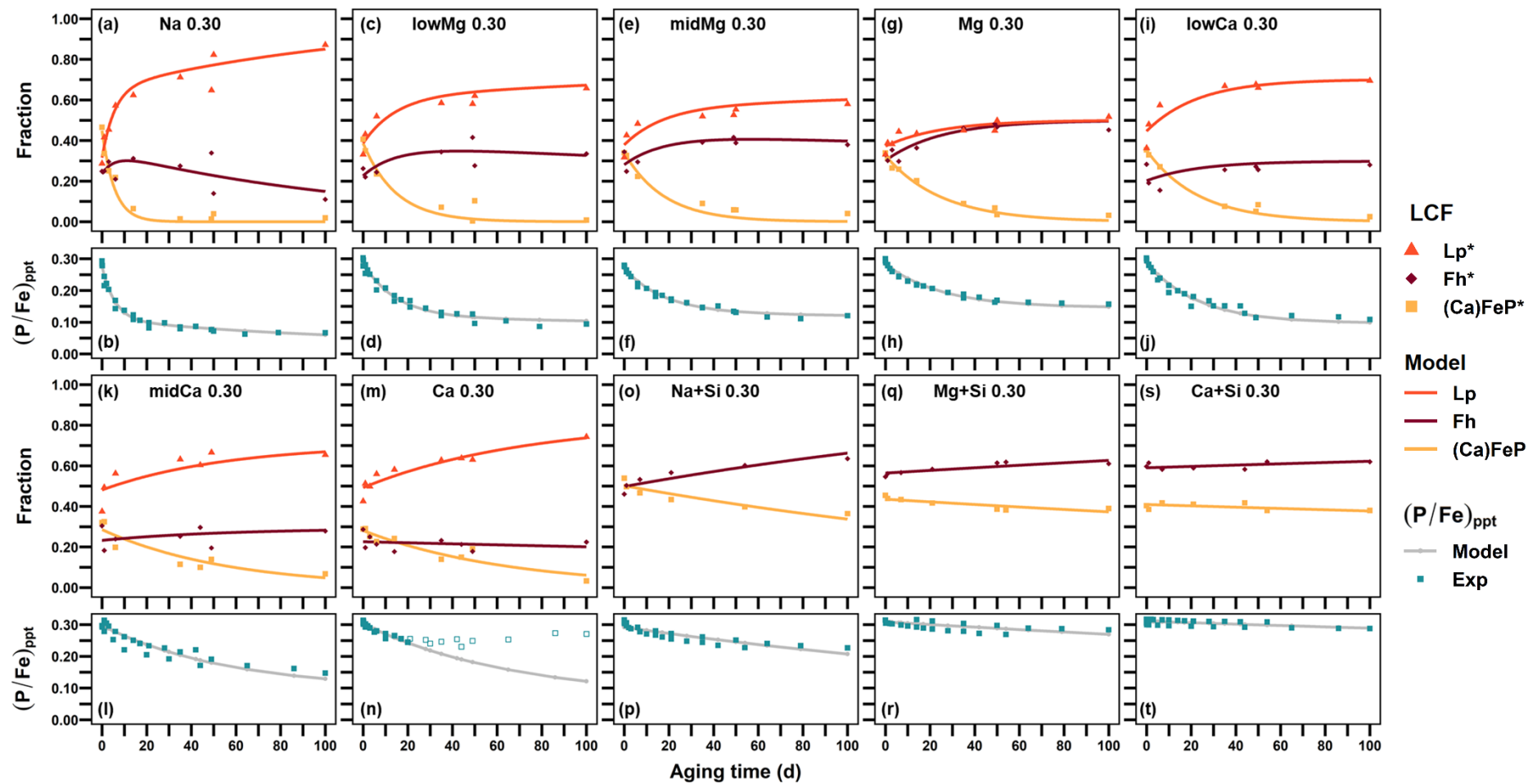


**Figure S12.** Experimental and modelled Fe(III)-precipitate fractions and solution-derived  $(P/Fe)_{ppt}$  as a function of aging time for the treatments Na 0.30 (a, b), lowMg 0.30 (c, d), midMg 0.30 (e, f), Mg 0.30 (g, h), lowCa 0.30 (i, j), midCa 0.30 (k, l), Ca 0.30 (m, n), Na+Si 0.30 (o, p), Mg+Si 0.30 (q, r), Ca+Si 0.30 (s, t). Experimental data (symbols) and model calculations (lines). Model calculations based on first-order transformation kinetics for  $(Ca)FeP^*$  into  $Fh^*$ ,  $(Ca)FeP^*$  into  $Lp^*$ , and for  $Fh^*$  into  $Lp^*$ , and on constant  $(P/Fe)$  for each precipitate fraction. Fit parameters are listed in Table 3.

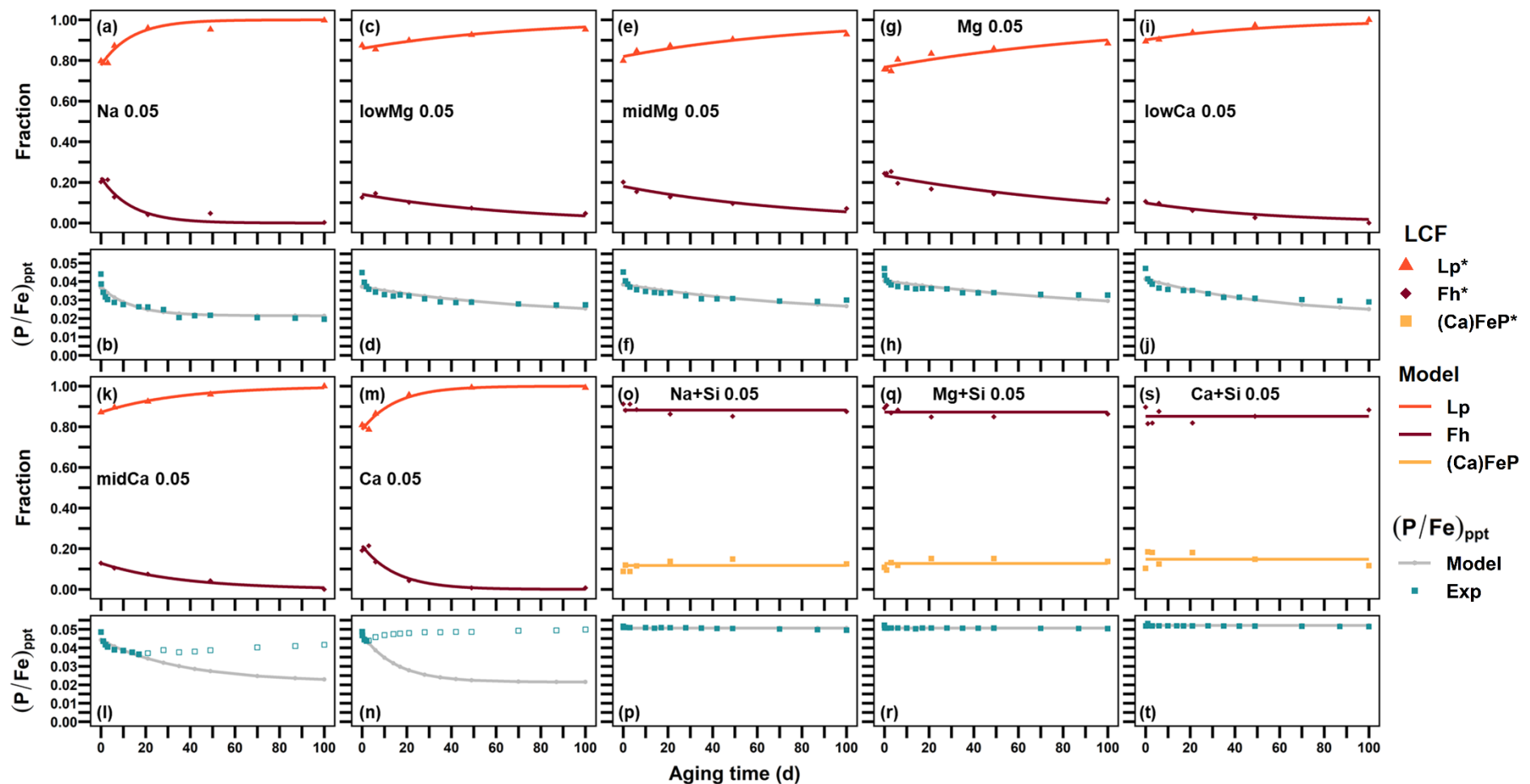


**Figure S13.** Experimental and modelled Fe(III)-precipitate fractions and solution-derived  $(P/Fe)_{ppt}$  as a function of aging time for the treatments Na 0.05 (a, b), lowMg 0.05 (c, d), midMg 0.05 (e, f), Mg 0.05 (g, h), lowCa 0.05 (i, j), midCa 0.05 (k, l), Ca 0.05 (m, n), Na+Si 0.05 (o, p), Mg+Si 0.05 (q, r), Ca+Si 0.05 (s, t). Experimental data (symbols) and model calculations (lines). Model calculations based on first-order transformation kinetics for  $(Ca)FeP^*$  into  $Fh^*$ ,  $(Ca)FeP^*$  into  $Lp^*$ , and for  $Fh^*$  into  $Lp^*$ , and on constant  $(P/Fe)$  for each precipitate fraction. Fit parameters are listed in Table 3.

## 7 Transmission electron microscopy

### 7.1 Secondary electron and high-angle annular dark field images

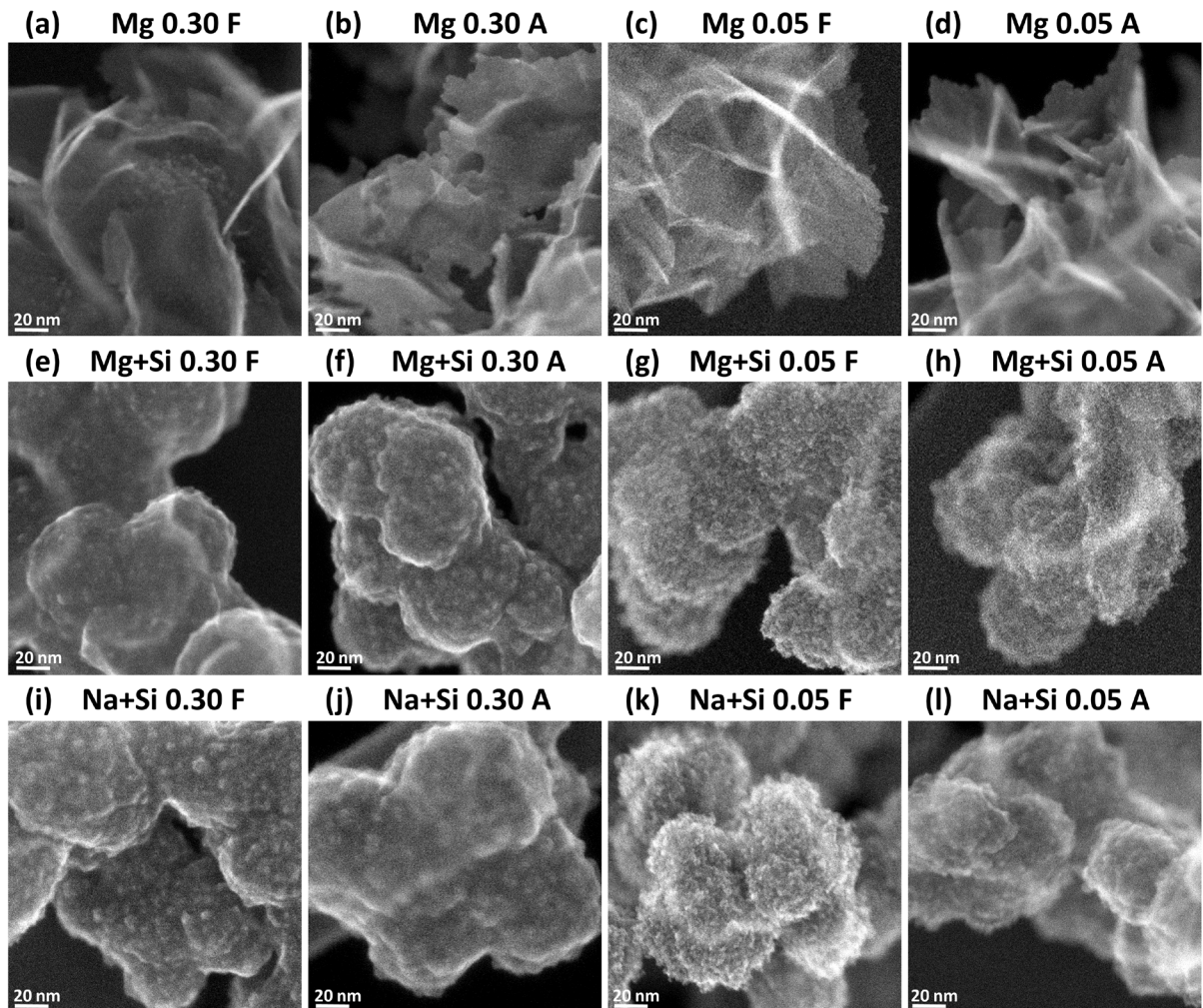


**Figure S14.** Secondary electron (SE) images showing the morphology of Fe(III)-precipitates freshly formed (F) and 100-d aged (A) in (a-d) Mg, (e-h) Mg+Si, and (i-l) Na+Si electrolytes at  $(P/Fe)_{init}$  of 0.30 or 0.05. Corresponding high-angle annular dark-field (HAADF) images depicting the sample density are shown in Fig. S16.

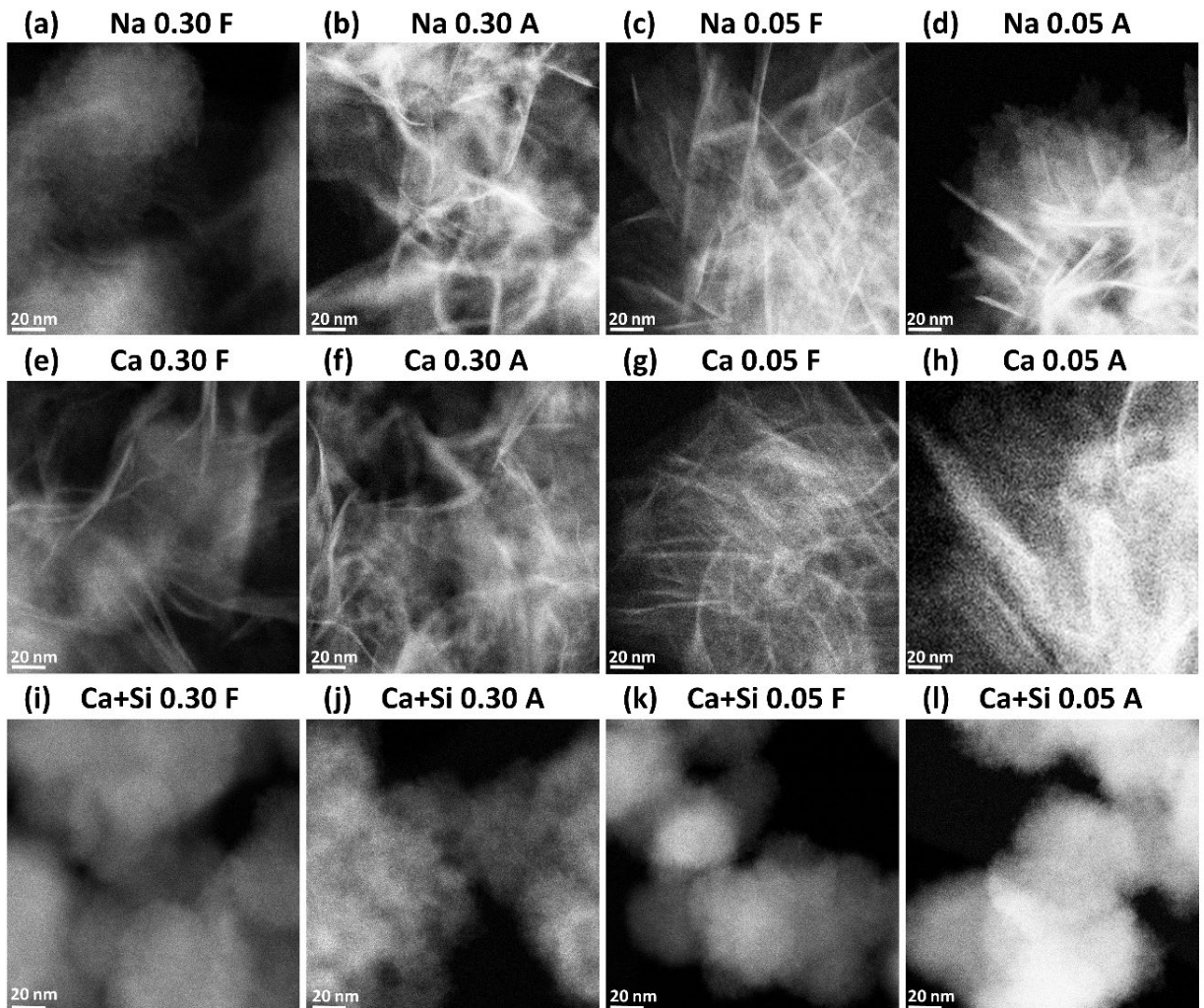


**Figure S15.** High-angle annular dark-field (HAADF) images showing the density of Fe(III)-precipitates freshly formed (F) and 100-d aged (A) in (a-d) Na, (e-h) Ca, and (i-l) Ca+Si electrolytes at  $(P/Fe)_{init}$  of 0.30 or 0.05. Corresponding SE images are shown in Fig. 8.

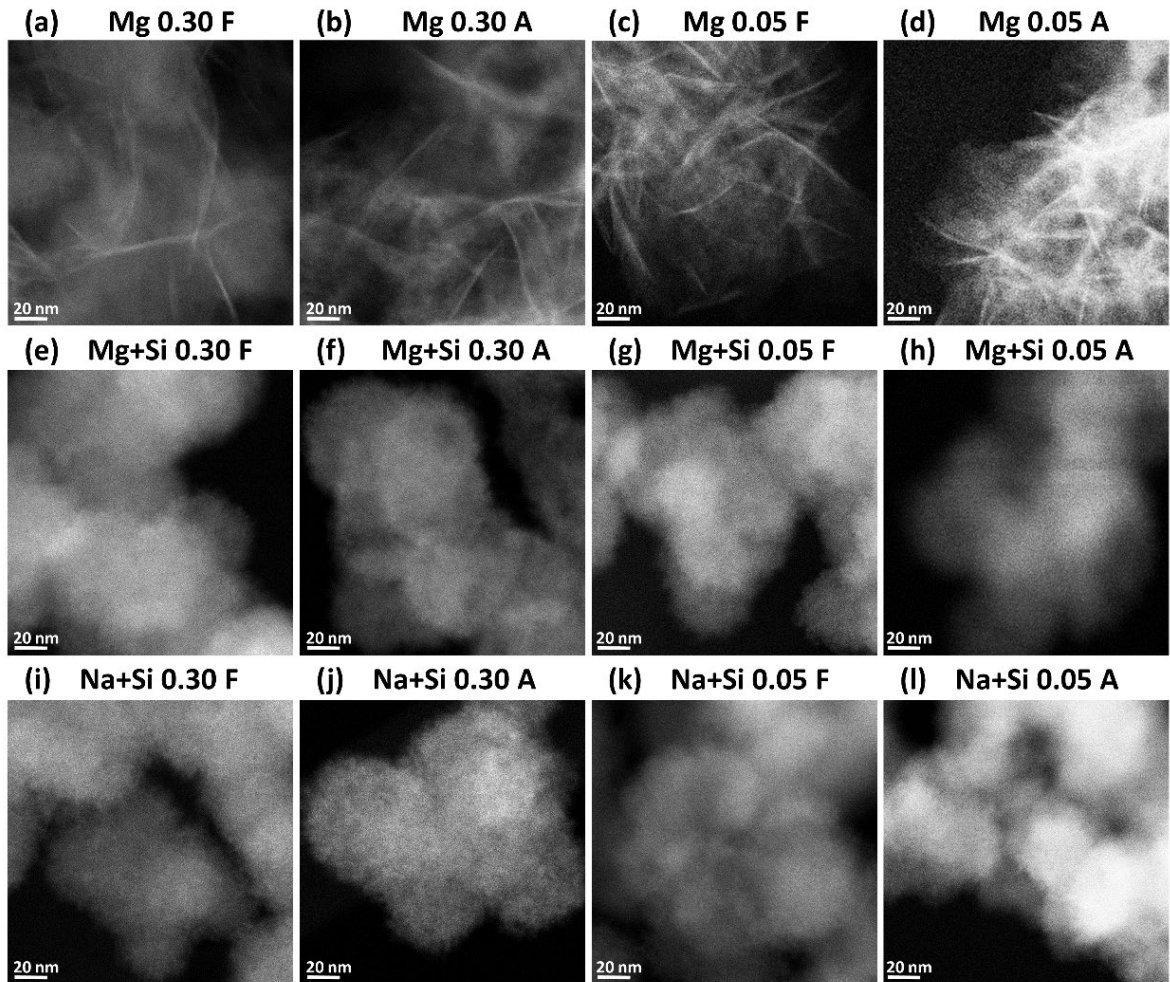


**Figure S16.** High-angle annular dark-field (HAADF) images showing the density of Fe(III)-precipitates freshly formed (F) and 100-d aged (A) in (a-d) Mg, (e-h) Mg+Si, and (i-l) Na+Si electrolytes at  $(P/Fe)_{init}$  of 0.30 or 0.05.

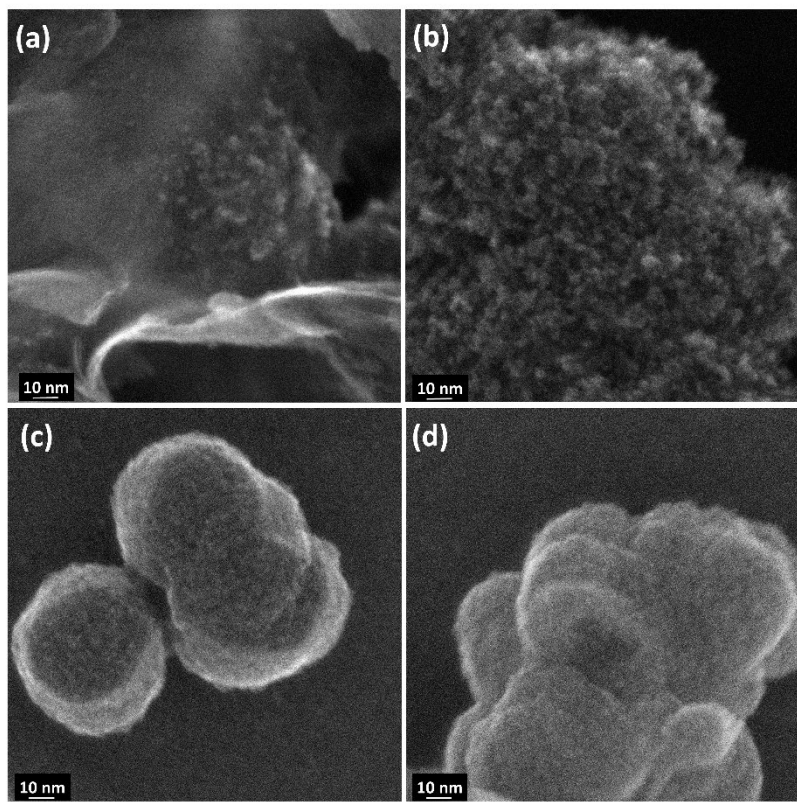


**Figure S17.** Comparison of secondary electron (SE) images at higher magnification of (a) fresh Fe(III)-precipitate surface at Na 0.30, (b) fresh Si-ferrihydrite (Na+Si; Si/Fe 1.0, P/Fe 0), (c) fresh amorphous Fe(III)-phosphate (Na; P/Fe 1.0), and (d) fresh amorphous Ca-Fe(III)-phosphate (Ca; P/Fe 1.0).

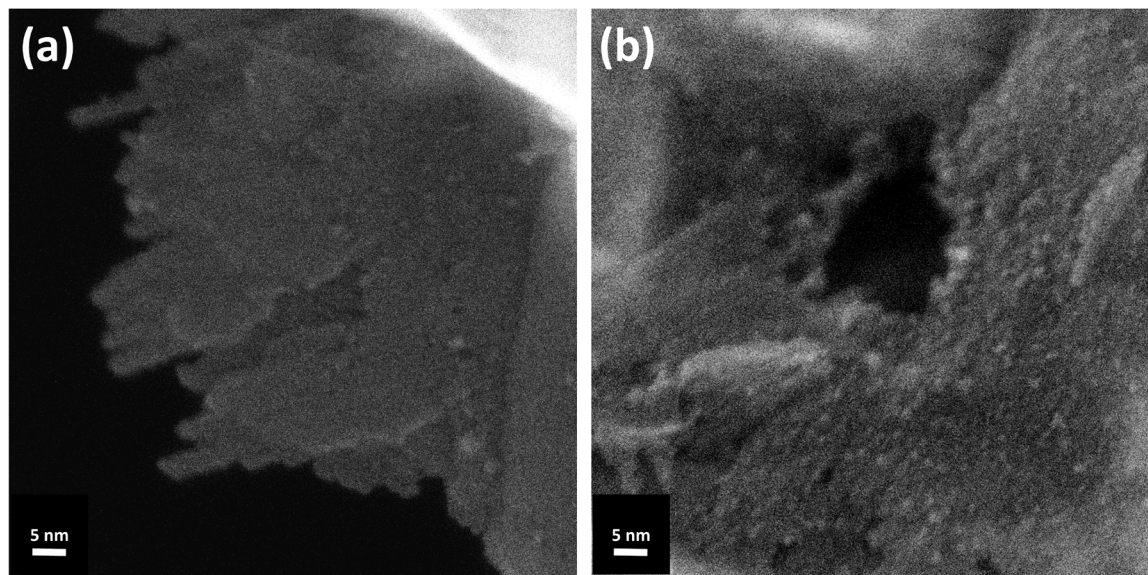


**Figure S18.** Comparison of secondary electron (SE) images at higher magnification of Fe(III)-precipitates aged for 100 d in the (a) Na and (b) Mg electrolytes at  $(P/Fe)_{init}$  of 0.30.

## 7.2 STEM-EDX results

Fresh and aged precipitates from Na, Mg, Ca, Na+Si, Mg+Si, and Ca+Si electrolytes at  $(P/Fe)_{init}$  0.30 and 0.05 were analyzed with STEM-EDX. For EDX data evaluation, including the extraction of element distribution maps for Fe, Ca, P, and Si, and the calculation of element ratios over selected sample areas based on a fundamental parameter approach, the software code Velox was used (ThermoFischer Scientific). Elemental ratios derived from the cumulative EDX spectra over the entire image range were considered to represent the bulk elemental ratios. For  $\text{SiO}_4$  free electrolytes, three integrated areas were selected from areas comprising either Lp or (Ca-)Fe(III)-phosphate. For  $\text{SiO}_4$  containing electrolytes, Fh instead of Lp was assumed as a structural component. Examples of EDX area selection in fresh Na 0.30 and Na+Si 0.30 are presented in Fig. S20. The ratios tabulated in Tables S10 and S11 represent averaged values from three areas. The EDX spectral quantification was achieved with a least-squares empirical fit of spectra. Certain elements (O, C, Cu, K, Mo, Al) were quantified with deconvolution only, subtracting their peaks in case of a peak overlap with elements of interest, allowing more accurate element quantification.

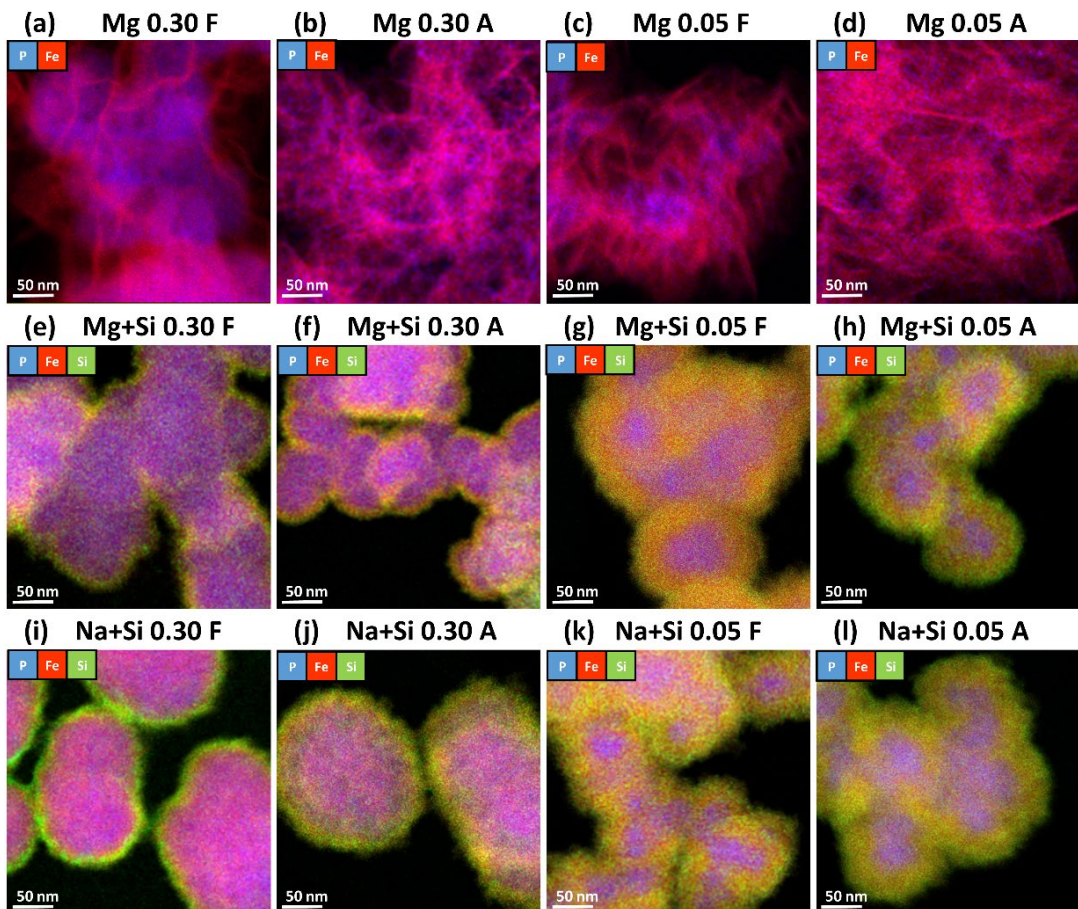


**Figure S19.** Energy-dispersive X-ray (EDX) elemental maps of Fe-precipitates freshly formed (F) and 100-d aged (A) in (a-d) Mg, (e-h) Mg+Si, and (i-l) Na+Si electrolytes at  $(P/Fe)_{init}$  of 0.30 or 0.05. Elemental ratios obtained by EDX-analysis are listed in Tables S10 and S11.

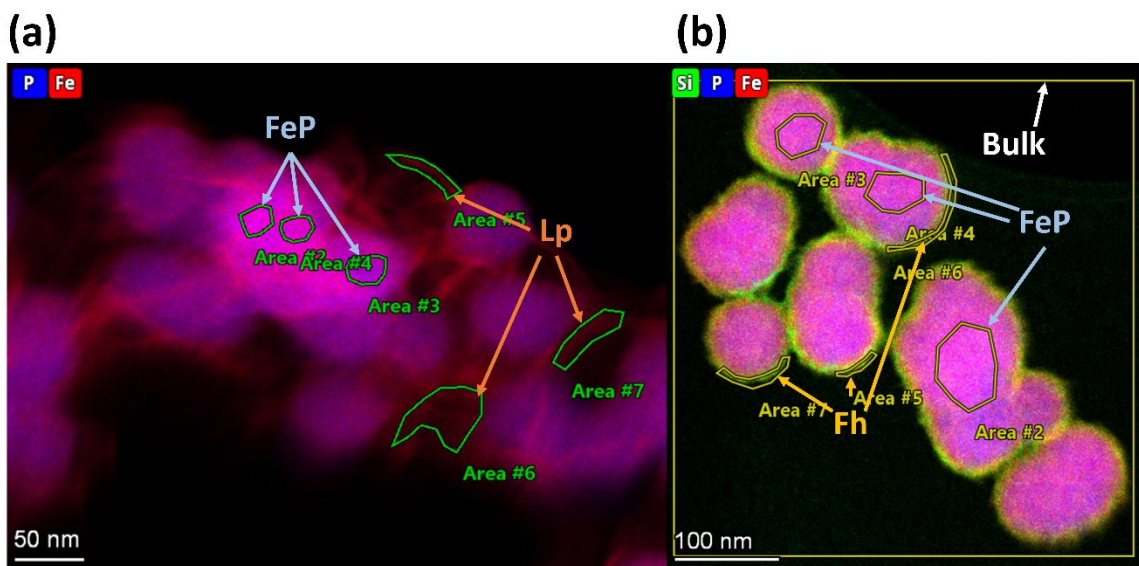


**Figure S20.** An example of an EDX area selection. (a) Na 0.30 0d, with FeP and Lp (b) Na+Si 0.30 0d, with FeP, Fh, and full area (bulk).

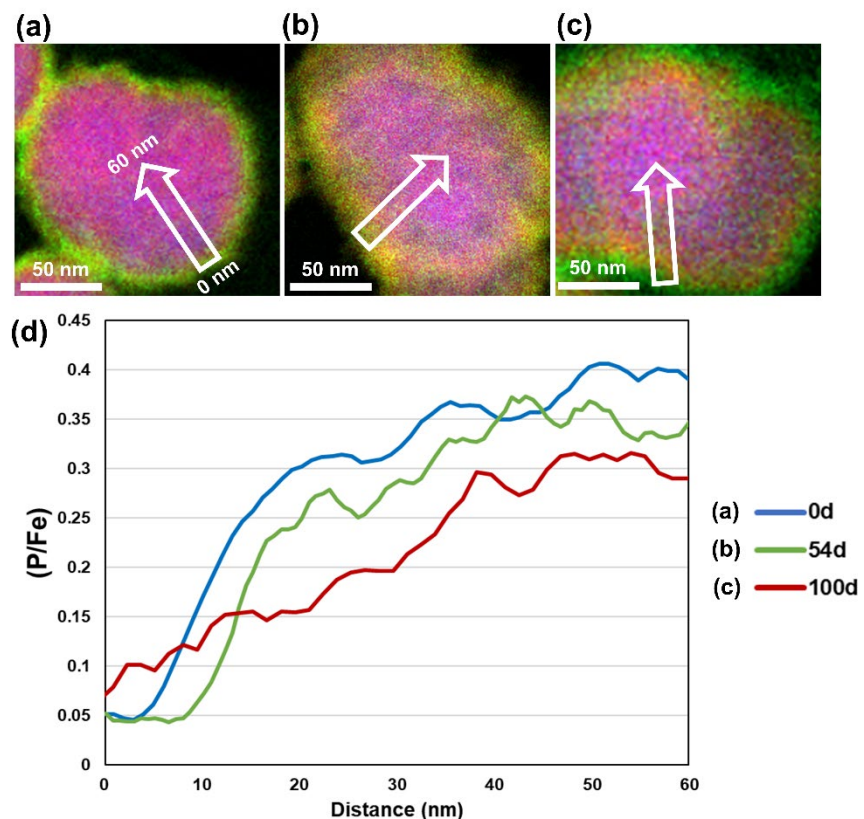


**Figure S21.** Individual FeP/Fh particle and EDX line profile (white arrow) in (a) Na+Si 0.30 0d, (b) Na+Si 0.30 54d, (c) Na+Si 0.30 100d, (d) P/Fe derived from EDX atomic fraction of Fe and P across the line profile from the center to the edge of a FeP/Fh particle.

**Table S10.** EDX-derived elemental ratios of precipitates formed and aged at  $(\text{P}/\text{Fe})_{\text{init}} = 0.30$ . Values indicate average ( $\pm$  standard deviation) of values from three integrated areas for each structural component.

Electrolyte	(d)	Bulk			Lp			FeP			CaP P/Ca
		P/Fe	(Ca,Mg)/Fe	Si/Fe	P/Fe	(Ca,Mg)/Fe	Si/Fe	P/Fe	(Ca,Mg)/Fe	Si/Fe	
Na	0	0.28	-	-	0.06 ( $\pm 0.00$ )	-	-	0.43 ( $\pm 0.02$ )	-	-	-
	49	0.08	-	-	0.07 ( $\pm 0.00$ )	-	-	NI <sup>a</sup>	-	-	-
	100	0.05	-	-	0.05 ( $\pm 0.00$ )	-	-	NI <sup>a</sup>	-	-	-
Mg	0	0.28	0.11	-	0.04 ( $\pm 0.00$ )	0.04 ( $\pm 0.00$ )	-	0.64 ( $\pm 0.08$ )	0.19 ( $\pm 0.02$ )	-	-
	49	-	-	-	-	-	-	-	-	-	-
	100	0.14	0.08	-	0.15 ( $\pm 0.01$ )	0.08 ( $\pm 0.00$ )	-	NI <sup>a</sup>	NI <sup>a</sup>	-	-
Ca	0	0.29	0.41	-	0.05 ( $\pm 0.00$ )	0.22 ( $\pm 0.00$ )	-	0.71 ( $\pm 0.03$ )	0.53 ( $\pm 0.00$ )	-	-
	49	0.30	0.22	-	0.08 ( $\pm 0.00$ )	0.05 ( $\pm 0.00$ )	-	0.60 ( $\pm 0.01$ )	0.42 ( $\pm 0.00$ )	-	-
	100	0.21	0.21	-	0.09 ( $\pm 0.01$ )	0.05 ( $\pm 0.01$ )	-	NI <sup>a</sup>	NI <sup>a</sup>	-	0.72 ( $\pm 0.02$ )
		Bulk			Fh			FeP			CaCO <sub>3</sub>
Na+Si	0	0.26	-	0.13	0.04 ( $\pm 0.01$ )	-	0.33 ( $\pm 0.00$ )	0.36 ( $\pm 0.02$ )	-	0.06 ( $\pm 0.00$ )	-
	54	0.22	-	0.15	0.05 ( $\pm 0.00$ )	-	0.21 ( $\pm 0.00$ )	0.36 ( $\pm 0.03$ )	-	0.10 ( $\pm 0.01$ )	-
	100	0.21	-	0.54 <sup>b</sup>	0.07 ( $\pm 0.02$ )	-	0.60 ( $\pm 0.21$ ) <sup>b</sup>	0.32 ( $\pm 0.03$ )	-	0.18 ( $\pm 0.01$ ) <sup>b</sup>	-
Mg+Si	0	0.32	0.08	0.06	0.05 ( $\pm 0.00$ )	0.02 ( $\pm 0.00$ )	0.12 ( $\pm 0.01$ )	0.42 ( $\pm 0.01$ )	0.11 ( $\pm 0.00$ )	0.05 ( $\pm 0.00$ )	-
	54	0.25	0.11	0.13	0.05 ( $\pm 0.01$ )	0.05 ( $\pm 0.00$ )	0.21 ( $\pm 0.02$ )	0.42 ( $\pm 0.02$ )	0.16 ( $\pm 0.01$ )	0.08 ( $\pm 0.01$ )	-
	100	0.25	0.09	0.09	0.06 ( $\pm 0.02$ )	0.05 ( $\pm 0.00$ )	0.14 ( $\pm 0.01$ )	0.41 ( $\pm 0.02$ )	0.12 ( $\pm 0.01$ )	0.06 ( $\pm 0.00$ )	-
Ca+Si	0	0.31	0.17	0.08	0.07 ( $\pm 0.02$ )	0.05 ( $\pm 0.02$ )	0.15 ( $\pm 0.03$ )	0.59 ( $\pm 0.01$ )	0.22 ( $\pm 0.01$ )	0.04 ( $\pm 0.00$ )	-
	54	0.30	0.10	0.12	0.07 ( $\pm 0.01$ )	0.05 ( $\pm 0.00$ )	0.20 ( $\pm 0.01$ )	0.54 ( $\pm 0.06$ )	0.16 ( $\pm 0.01$ )	0.07 ( $\pm 0.01$ )	-
	100	0.28	0.16	0.20	0.10 ( $\pm 0.01$ )	0.09 ( $\pm 0.01$ )	0.31 ( $\pm 0.01$ )	0.47 ( $\pm 0.01$ )	0.24 ( $\pm 0.01$ )	0.13 ( $\pm 0.01$ )	0.0054 ( $\pm 0.004$ )

<sup>a</sup>phase not identified with STEM-EDX. <sup>b</sup>Si contamination during the STEM-EDX measurement.

**Table S11.** EDX-derived elemental ratios of precipitates formed and aged at  $(\text{P}/\text{Fe})_{\text{init}} = 0.05$ . Values indicate average ( $\pm$  standard deviation) of values from three integrated areas for each structural component.

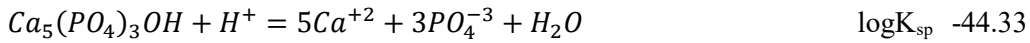
Electrolyte	(d)	Bulk			Lp			Fh			CaCO <sub>3</sub>	
		P/Fe	(Ca,Mg)/Fe	Si/Fe	P/Fe	(Ca,Mg)/Fe	Si/Fe	P/Fe	(Ca,Mg)/Fe	Si/Fe	P/Ca	
<b>Na</b>	0	0.06	-	-	0.05 ( $\pm 0.00$ )	-	-	0.16 ( $\pm 0.01$ )	-	-	-	-
	100	0.03	-	-	0.03 ( $\pm 0.00$ )	-	-	NI <sup>a</sup>	-	-	-	-
<b>Mg</b>	0	0.06	0.00	-	0.05 ( $\pm 0.00$ )	0.00 ( $\pm 0.00$ )	-	0.17 ( $\pm 0.02$ )	0.00 ( $\pm 0.00$ )	-	-	-
	100	0.03	0.02	-	0.03 ( $\pm 0.00$ )	0.02 ( $\pm 0.00$ )	-	NI <sup>a</sup>	NI <sup>a</sup>	-	-	-
<b>Ca</b>	0	0.06	0.01	-	0.04 ( $\pm 0.01$ )	0.00 ( $\pm 0.00$ )	-	0.22 ( $\pm 0.02$ )	0.04 ( $\pm 0.00$ )	-	-	-
	100	0.02	0.00	-	0.02 ( $\pm 0.00$ )	0.00 ( $\pm 0.00$ )	-	NI <sup>a</sup>	NI <sup>a</sup>	-	0.0047 ( $\pm 0.0013$ )	
		Bulk			Fh			FeP			CaCO <sub>3</sub>	
<b>Na+Si</b>	0	0.06	-	0.12	0.02 ( $\pm 0.00$ )	-	0.16 ( $\pm 0.01$ )	0.21 ( $\pm 0.02$ )	-	0.07 ( $\pm 0.00$ )	-	-
	100	0.05	-	0.22	0.00 ( $\pm 0.00$ )	-	0.28 ( $\pm 0.01$ )	0.16 ( $\pm 0.00$ )	-	0.17 ( $\pm 0.01$ )	-	-
<b>Mg+Si</b>	0	0.06	0.04	0.10	0.02 ( $\pm 0.00$ )	0.02 ( $\pm 0.00$ )	0.14 ( $\pm 0.00$ )	0.22 ( $\pm 0.02$ )	0.08 ( $\pm 0.01$ )	0.07 ( $\pm 0.00$ )	-	-
	100	0.05	0.03	0.22	0.00 ( $\pm 0.00$ )	0.02 ( $\pm 0.02$ )	0.29 ( $\pm 0.00$ )	0.17 ( $\pm 0.01$ )	0.04 ( $\pm 0.01$ )	0.14 ( $\pm 0.00$ )	-	-
<b>Ca+Si</b>	0	0.05	0.08	0.12	0.02 ( $\pm 0.01$ )	0.06 ( $\pm 0.00$ )	0.13 ( $\pm 0.00$ )	0.25 ( $\pm 0.01$ )	0.19 ( $\pm 0.01$ )	0.08 ( $\pm 0.01$ )	-	-
	100	0.04	0.06	0.23	0.01 ( $\pm 0.00$ )	0.05 ( $\pm 0.00$ )	0.26 ( $\pm 0.00$ )	0.18 ( $\pm 0.02$ )	0.13 ( $\pm 0.02$ )	0.18 ( $\pm 0.00$ )	0.0004 ( $\pm 0.0001$ )	

<sup>a</sup>phase not identified with STEM-EDX.

## 8 Calculation of saturation indices for Ca-phosphates and calcite

For the Ca-containing treatments, the saturation indices (SI) of Ca-phosphates and calcite were calculated based on the measured pH and dissolved Ca and P concentrations. The concentration of bicarbonate, the dominant form of dissolved inorganic carbon in the experimental pH range, was estimated by assuming that bicarbonate compensated the charge of dissolved Na and Ca (i.e., assuming that Ca removal was exclusively due to  $\text{CaCO}_3$  precipitation, and neglecting Na added with the  $\text{PO}_4$  and  $\text{SiO}_4$  stocks). Constants for phosphate protonation, dissolved  $\text{CaHPO}_4$  and  $\text{CaPO}_4^-$  complex formation, and the solubility products of hydroxyapatite (HAP), brushite, monetite and calcite were taken from the MinteqA2 V4 database as provided with the PHREEQC software (Parkhurst and Appelo., 1999); the solubility product of octacalcium phosphate (OCP;  $\log K_{\text{sp}}$  47.08) was taken from (Tung et al., 1988),  $\beta$ -tricalcium phosphate ( $\beta$ -TCP;  $\log K_{\text{sp}}$  28.92) from (Gregory et al., 1974), and the solubility product of amorphous calcium-phosphate (ACP;  $\log K_{\text{sp}}$  25.5) was taken from (Christoffersen et al., 1990). The Davies equation was used for the calculation of the activity coefficients of mono-, di- and trivalent ions, based on the ionic strength estimated from the nominal concentrations of Na and Ca and with bicarbonate as charge-balancing anion.

HAP



$\beta$ -TCP



OCP



ACP



Brushite



Monetite



Calcite



**Table S12.** Dissolved Ca and P, suspension pH in Ca-containing electrolytes at  $(P/Fe)_{init}$  0.30 and saturation indices (SI) for hydroxyapatite (HAP),  $\beta$ -tricalcium-phosphate ( $\beta$ -TCP), octacalcium-phosphate (OCP), amorphous calcium phosphate (ACP), and calcite. The underlined values indicate supersaturation of the respective phase in the given sample. Brushite and monetite remained undersaturated in all treatments.

Treatment	Time (d)	Ca mM	P mM	pH	SI				
					HAP	$\beta$ -TCP	OCP	ACP	Calcite
Ca 0.30	0	3.706	0.003	7.2	<u>4.7</u>	-1.4	-4.4	-4.8	<u>0.5</u>
	1	3.653	0.009	7.9	<u>9.2</u>	<u>1.1</u>	-1.3	-2.3	<u>1.2</u>
	5	3.635	0.017	8.0	<u>10.2</u>	<u>1.7</u>	-0.4	-1.7	<u>1.3</u>
	10	3.627	0.027	7.9	<u>10.5</u>	<u>2.0</u>	<u>0.1</u>	-1.4	<u>1.2</u>
	20	3.652	0.032	8.0	<u>11.2</u>	<u>2.4</u>	<u>0.5</u>	-1.0	<u>1.3</u>
	30	3.632	0.034	7.8	<u>10.5</u>	<u>2.0</u>	<u>0.2</u>	-1.4	<u>1.1</u>
	44	3.637	0.039	8.1	<u>11.7</u>	<u>2.7</u>	<u>0.9</u>	-0.8	<u>1.4</u>
	65	3.606	0.028	8.3	<u>11.8</u>	<u>2.6</u>	<u>0.7</u>	-0.8	<u>1.5</u>
	86	3.469	0.018	8.2	<u>10.9</u>	<u>2.1</u>	<u>0.0</u>	-1.3	<u>1.4</u>
	100	3.365	0.020	8.2	<u>10.9</u>	<u>2.1</u>	<u>0.0</u>	-1.3	<u>1.3</u>
midCa 0.30	0	1.094	0.004	7.2	<u>3.1</u>	-2.4	-5.5	-5.8	<u>0.0</u>
	1	1.022	0.013	8.1	<u>8.0</u>	<u>0.4</u>	-2.2	-3.0	<u>0.8</u>
	5	1.058	0.025	8.2	<u>9.4</u>	<u>1.2</u>	-1.1	-2.2	<u>1.0</u>
	10	1.048	0.040	8.1	<u>9.8</u>	<u>1.5</u>	-0.6	-1.9	<u>0.9</u>
	20	1.049	0.047	8.2	<u>10.3</u>	<u>1.8</u>	-0.2	-1.6	<u>1.0</u>
	30	1.042	0.053	8.1	<u>10.1</u>	<u>1.7</u>	-0.2	-1.7	<u>0.9</u>
	44	1.073	0.063	8.3	<u>11.1</u>	<u>2.3</u>	<u>0.4</u>	-1.1	<u>1.1</u>
	65	1.094	0.063	8.3	<u>11.3</u>	<u>2.4</u>	<u>0.5</u>	-1.0	<u>1.1</u>
	86	1.069	0.068	8.4	<u>11.7</u>	<u>2.6</u>	<u>0.8</u>	-0.8	<u>1.2</u>
	100	1.081	0.074	8.4	<u>11.9</u>	<u>2.7</u>	<u>0.9</u>	-0.7	<u>1.2</u>
lowCa 0.30	0	0.341	0.006	7.3	<u>1.3</u>	-3.4	-6.9	-6.8	-0.4
	1	0.311	0.017	8.1	<u>6.0</u>	-0.8	-3.7	-4.2	<u>0.3</u>
	5	0.327	0.038	8.2	<u>7.9</u>	<u>0.3</u>	-2.2	-3.1	<u>0.5</u>
	10	0.328	0.058	8.2	<u>8.5</u>	<u>0.7</u>	-1.6	-2.7	<u>0.5</u>
	20	0.338	0.078	8.3	<u>9.1</u>	<u>1.1</u>	-1.1	-2.3	<u>0.6</u>
	30	0.336	0.077	8.3	<u>9.0</u>	<u>1.1</u>	-1.1	-2.3	<u>0.6</u>
	44	0.339	0.089	8.3	<u>9.5</u>	<u>1.4</u>	-0.8	-2.1	<u>0.6</u>
	65	0.344	0.092	8.4	<u>9.7</u>	<u>1.5</u>	-0.6	-1.9	<u>0.7</u>
	86	0.347	0.094	8.5	<u>10.2</u>	<u>1.7</u>	-0.4	-1.7	<u>0.8</u>
	100	0.345	0.098	8.5	<u>10.3</u>	<u>1.8</u>	-0.3	-1.7	<u>0.8</u>
Ca+Si 0.30	0	3.691	0.000	7.0	-0.2	-4.6	-8.9	-8.0	<u>0.3</u>
	1	3.580	0.000	7.9	<u>4.9</u>	-1.7	-5.4	-5.1	<u>1.1</u>
	5	3.184	0.001	7.7	<u>5.1</u>	-1.5	-4.9	-4.9	<u>0.9</u>
	10	2.932	0.002	7.7	<u>5.9</u>	-1.0	-4.1	-4.4	<u>0.8</u>
	20	2.842	0.003	7.8	<u>6.4</u>	-0.6	-3.6	-4.1	<u>0.8</u>
	30	2.783	0.003	7.7	<u>6.6</u>	-0.5	-3.3	-3.9	<u>0.8</u>
	44	2.776	0.004	7.8	<u>7.2</u>	-0.1	-3.0	-3.6	<u>0.8</u>
	65	2.625	0.005	7.9	<u>7.5</u>	<u>0.1</u>	-2.7	-3.4	<u>0.8</u>
	86	2.572	0.006	7.9	<u>8.0</u>	<u>0.4</u>	-2.3	-3.1	<u>0.9</u>
	100	2.471	0.006	7.9	<u>8.0</u>	<u>0.3</u>	-2.3	-3.1	<u>0.8</u>

**Table S13.** Dissolved Ca and P, suspension pH in Ca-containing electrolytes at  $(P/Fe)_{init}$  0.05 and saturation indices (SI) for hydroxyapatite (HAP),  $\beta$ -tricalcium-phosphate ( $\beta$ -TCP), octacalcium-phosphate (OCP), amorphous calcium phosphate (ACP), and calcite. The underlined values indicate supersaturation of the respective phase in the given sample. Brushite and monetite remained undersaturated in all treatments.

Treatment	Time (d)	Ca mM	P mM	pH	SI				
					HAP	$\beta$ -TCP	OCP	ACP	Calcite
<b>Ca 0.05</b>	0	4.003	0.001	6.9	<u>2.1</u>	-3.0	-6.3	-6.4	0.2
	1	4.024	0.003	7.4	<u>6.0</u>	-0.7	-3.5	-4.1	0.8
	3	3.438	0.004	7.5	<u>6.0</u>	-0.7	-3.5	-4.2	0.7
	6	3.256	0.003	7.4	<u>5.3</u>	-1.2	-4.1	-4.6	0.6
	10	3.189	0.002	7.2	<u>4.0</u>	-1.9	-5.0	-5.3	0.4
	21	2.846	0.002	7.4	<u>4.3</u>	-1.8	-5.0	-5.2	0.4
	35	2.715	0.001	7.1	<u>2.6</u>	-2.7	-6.1	-6.1	0.1
	49	2.586	0.001	7.4	<u>3.9</u>	-2.0	-5.4	-5.5	0.4
	70	2.347	0.001	7.3	<u>2.8</u>	-2.7	-6.2	-6.1	0.1
	100	1.896	0.001	7.5	<u>3.2</u>	-2.6	-6.2	-6.0	0.2
<b>midCa 0.05</b>	0	1.125	0.002	7.0	<u>0.8</u>	-3.7	-7.4	-7.2	-0.2
	1	1.106	0.004	7.9	<u>6.0</u>	-0.8	-3.9	-4.3	0.7
	3	1.030	0.006	7.9	<u>6.3</u>	-0.6	-3.5	-4.0	0.6
	6	1.043	0.006	7.8	<u>6.0</u>	-0.8	-3.7	-4.2	0.6
	10	1.056	0.007	7.9	<u>6.6</u>	-0.5	-3.3	-3.9	0.7
	21	1.051	0.007	7.9	<u>6.7</u>	-0.4	-3.2	-3.8	0.7
	35	1.002	0.007	7.7	<u>5.6</u>	-1.0	-3.9	-4.4	0.4
	49	0.912	0.007	8.0	<u>6.5</u>	-0.5	-3.4	-3.9	0.7
	70	0.738	0.006	7.9	<u>5.8</u>	-1.0	-4.0	-4.4	0.5
	100	0.522	0.005	8.1	<u>5.7</u>	-1.1	-4.3	-4.5	0.6
<b>lowCa 0.05</b>	0	0.388	0.002	7.0	-1.1	-4.8	-8.7	-8.2	-0.6
	1	0.382	0.005	8.0	<u>4.8</u>	-1.6	-4.9	-5.0	0.4
	3	0.356	0.007	8.0	<u>4.8</u>	-1.6	-4.8	-5.0	0.3
	6	0.388	0.008	8.0	<u>5.3</u>	-1.2	-4.4	-4.7	0.4
	10	0.374	0.008	8.1	<u>5.5</u>	-1.2	-4.3	-4.6	0.4
	21	0.351	0.008	8.2	<u>5.9</u>	-1.0	-4.1	-4.4	0.5
	35	0.391	0.010	8.0	<u>5.8</u>	-1.0	-4.0	-4.4	0.4
	49	0.382	0.010	8.3	<u>6.7</u>	-0.5	-3.5	-3.9	0.6
	70	0.383	0.011	8.3	<u>7.1</u>	-0.3	-3.3	-3.7	0.7
	100	0.364	0.011	8.5	<u>7.8</u>	0.1	-2.9	-3.3	0.9
<b>Ca+Si 0.05</b>	0	3.495	0.000	6.7	-3.0	-6.2	-11.0	-9.7	-0.1
	1	3.893	0.000	7.7	<u>1.4</u>	-3.9	-8.5	-7.3	1.0
	3	3.153	0.000	7.5	<u>1.2</u>	-4.0	-8.4	-7.4	0.7
	6	2.695	0.000	7.4	-0.1	-4.7	-9.5	-8.2	0.4
	10	2.806	0.000	7.6	<u>0.9</u>	-4.2	-8.8	-7.6	0.6
	21	2.378	0.000	7.5	<u>0.4</u>	-4.4	-8.9	-7.8	0.3
	35	2.269	0.000	7.5	<u>0.6</u>	-4.3	-8.8	-7.7	0.3
	49	2.125	0.000	7.5	<u>0.8</u>	-4.1	-8.6	-7.6	0.3
	70	1.912	0.000	7.6	<u>1.4</u>	-3.8	-8.1	-7.2	0.2
	100	1.601	0.000	7.6	<u>1.5</u>	-3.7	-7.8	-7.1	0.0

## 9 References

- Christoffersen, M., Christoffersen, J. and Kibalczyc, W. (1990) Apparent solubilities of two amorphous calcium phosphates and of octacalcium phosphate in the temperature range 30–42°C. *J. Cryst. Growth* 106, 349–354.
- Gregory, T., Moreno, E., Patel, J. and Brown, W. (1974) Solubility of  $\beta$ -Ca<sub>3</sub>(PO<sub>4</sub>)<sub>2</sub> in the system Ca(OH)<sub>2</sub>-H<sub>3</sub>PO<sub>4</sub>-H<sub>2</sub>O at 5, 15, 25, and 37°C. *J. Res. Natl. Bur. Stand. A Phys. Chem.* 78, 667.
- Parkhurst, D.L. and Appelo, C.A.J. (1999) User's Guide to PHREEQC (Version 2): A Computer Program for Speciation, Batch-Reaction, One-Dimensional Transport, and Inverse Geochemical Calculations. U.S. Geological Survey, Denver, CO.
- Tung, M., Eidelman, N., Sieck, B. and Brown, W. (1988) Octacalcium phosphate solubility product from 4 to 37°C. *J. Res. Natl. Bur. Stand.* 93, 613.